Investigation of the effect of blank holding force on Earing defect during circular deep drawing process through finite element analysis and experimentation using AA6061 and Low- carbon steel sheets

Amirela Siraji Sumeredin

A Thesis Submitted to

The department of Mechanical Design and Manufacturing Engineering

School of Mechanical, Chemical and Material Engineering

Presented in Partial Fulfillment of the Requirement for the Degree of Master's in Manufacturing Engineering

Office of Graduate Studies

Adama Science and Technology University

February, 2022

Adama, Ethiopia

Investigation of the effect of blank holding force on Earing defect during circular deep drawing process through finite element analysis and experimentation using AA6061 and Low- carbon steel sheets

Amirela Siraji Sumeredin

Advisor: Dr. Perumalla Janaki Ramulu

Co - Advisor: Dr. Habtamu B.

A thesis Submitted to

The department of Mechanical Design and Manufacturing Engineering

School of Mechanical, Chemical and Material Engineering

Presented in Partial Fulfillment of the Requirement for the Degree of Master's in Manufacturing Engineering

Office of Graduate Studies

Adama Science and Technology University

February, 2022

Adama, Ethiopia

Declaration

I hereby declare that this Master Thesis entitled "Investigation of the effect of blank holding force on Earing defect during circular deep drawing process through finite element analysis and experimentation using AA6061 and Low- carbon steel sheets" is my original work. That is, it has not been submitted for the award of any academic degree, diploma or certificate in any other university. All sources of materials that are used for this thesis have been duly acknowledged through citation

Name of student	Signature	Date

Approval Page of M.Sc. Thesis

I/we, the advisors of the thesis entitled "Investigation of the effect of blank holding force on Earing defect during circular deep drawing process through finite element analysis and experimentation using AA6061 and Low- carbon steel sheets" and developed by Amirela Siraji, hereby certify that the recommendation and suggestions made by the board of examiners are appropriately incorporated into the final version of the thesis.

____________________	____________________	____________________
Major Advisor	Signature	Date
____________________	____________________	____________________
Co-advisor	Signature	Date

We, the undersigned, members of the Board of Examiners of the thesis by Amirela Siraji have read and evaluated the thesis entitled "Investigation of the effect of blank holding force on Earing defect during circular deep drawing process through finite element analysis and experimentation and examined the candidate during open defense. This is, therefore, to certify that the thesis is accepted for partial fulfillment of the requirement of the degree of Master of Science in Manufacturing Engineering.

____________________	____________________	____________________
Chairperson	Signature	Date
____________________	____________________	____________________
Internal Examiner	Signature	Date
____________________	____________________	____________________
External Examiner	Signature	Date

Final approval and acceptance of the thesis is contingent upon submission of its final copy to the Office of Postgraduate Studies (OPGS) through the Department Graduate Council (DGC) and School Graduate Committee (SGC).

____________________	____________________	____________________
Department Head	Signature	Date
____________________	____________________	____________________
School Dean	Signature	Date
____________________	____________________	____________________
Office of Postgraduate Studies, Dean	Signature	Date

Recommendation

I/we, the advisor(s) of this thesis, hereby certify that I/we have read the revised version of the thesis entitled “Investigation of the effect of blank holding force on Earing defect during circular deep drawing process through finite element analysis and experimentation using AA6061 and Low- carbon steel sheets” prepared under my/our guidance by Amirela Siraji submitted in partial fulfillment of the requirements for the degree of Masters of Science in Manufacturing Engineering Therefore, I/we recommend the submission of revised version of the thesis to the department following the applicable procedures.

____________________	____________________	____________
Major Advisor	Signature	Date
____________________	____________________	____________
Co-advisor	Signature	Date

Acknowledgements

Foremost, I would like to express my sincere gratitude to my advisor Dr. Peremulu Janaki Ramulu for his continuous support of my MSc study and research, for his patience, motivation, enthusiasm, and immense knowledge. His guidance helped me in all the time of research and writing of this thesis. I could not have imagined having a better advisor and mentor for my MSc study.

Besides my advisor, I would like to thank the rest of my thesis committee: Dr. Habtamu, Dr. Moiera, and Dr. Gutata and also Mr. Mengistu Gelaw (Head of the Department) and Eliyas Habtu (Teacher) for their encouragement and insightful comments.

I would also like to thank to my colleague Tsegaye Bekele and Mukerim Ali, their support, suggestions and friendship made great contributions to this work.

I would also like to acknowledge ETU (Ethio-Technical University) for accepting me to present a conference paper titled “the effects of process parameters during deep drawing process through finite element analysis” and also thank Journal of Engineering whom provide me an opportunity to publish my paper titled “the relationship between earing and wrinkling defect during deep drawing process through finite element analysis” which is under-review to be published.

Table of Contents

List of tables

List of figures and illustration

List of Acronyms and Abbreviations

Symbol	Definition	Units
BHF/F_h	Blank holding force	kN
DR	Draw ratio	---
LDR	Limiting draw ratio	---
c	clearance	
WP 310	Gunt-humber model of UTM	
UTM	Universal testing machine	

Abstract

Earing is defined as the formation of waviness on uppermost portion of deep drawn cup. It is one of the major defects observed during deep drawing process. The objective of the present study aims to investigate the influence of the blank-holding force (BHF) on Earing defect in the deep-drawing process of cylindrical cups through finite element analysis and experimentation. For this purpose, Mechanical properties of AA6061 and low carbon steel sheets along with deep drawing tool design parameters were incorporated in the finite element modeling of deep drawing process. The finite element software (Pam-Stamp 2G) was utilized to carry out the numerical simulation of the deep drawing process. Different BHFs were applied during the deep drawing process. The simulation results showed that the best earing is observed when the BHF is 9kN for the AA6061 alloy and 20kN for the Low - Carbon steel sheet. The earing tendency and deep drawability of the low – carbon steel sheets is higher than AA6061.

Keywords: blank holding force, deep drawing, and PAMSTAMP

Chapter One

1. Introduction

1.1 Background of the study

Sheet metal forming is one of the most widely used manufacturing processes for making different kind of products in many industries. It is due to the ease with which metal may be formed into useful shapes through plastic deformation processes in which the volume and mass of the metal are conserved and the thickness is substantially the same as that of the original material. Deep drawing is one of the most important processes for forming sheet metal parts. It is mainly used for mass production of cup shapes in automobile, aerospace, and packaging industries. In deep drawing operation, a sheet metal (blank) converted to cylindrical parts by using a process in which sheet is drawn into cavity of die to convert the blank into desired (Ghosh A. and Mallik A, 2011). The deformation of a sheet metal in deep drawing was estimated quantitatively (Das et al., 2013; Nagda et al., 2017; Oluwole1* et al., 2010; Patel et al., 2015) using draw ratio (DR), which is defined as ratio of initial blank diameter to the diameter of the cup drawn from the blank (approximately equal to the punch diameter). For a given material there is a limiting draw ratio (LDR), representing the largest blank that can be drawn through a die without tearing (Ahmetoglu et al., 1992; Patel et al., 2015). Maximizing drawability in deep drawing operations directly reduces the manufacturing cost and time associated with these operations (Patel et al., 2015; Reddy et al., 2016). Furthermore, a prior knowledge of the limits of drawability can also be useful in avoiding the development of infeasible designs early on thereby decreasing the total product design cycle time. drawability can be increased by delaying the onset of process failures. Towards this end, process parameters which influence the drawing operation need to be properly selected. Blank shape is one of the most important process parameters that strongly influence drawability i.e., by altering the blank design considerable improvement in the drawability may be obtained (Patel et al., 2015). The quality of the product is influenced by the many of the process parameters like blank holder force, co-efficient of friction, strain rate, thickness, temperature, punch force and punch speed etc. So, a good knowledge is required to produce good quality of deep drawing products by minimizing the defects (JOSHI et al., 2013). One of the major defects(Singh et al., 2018) which affects the quality of the deep drawn cups is the occurrence of a wavy edge at the top, commonly referred to as the earing defect as shown in fig. 1.3. Earing is a result of non-uniform flow of material into the die cavity from different anisotropy directions of the sheet. The blank is anisotropic due to the directionality of plastic properties produced by rolling and other primary working process (Patel et al., 2015; Srirat et al., 2012). In practice, a significant amount of material is lost as this wavy edge of the cup needs to be trimmed. It is undesirable because it requires additional processing (Das et al., 2013). Information concerned formation of ears in deep drawing operation permits a pervious alteration of operation, which results in production of final cup with defect less/minimized and financial saving and time (Dixit, 2009; Han et al., 2013; Muhsin Younis * & Shbeeb Jaber, 2011; Nagda et al., 2017; Patel et al., 2015). Some research works have been conducted to explain the relationships between earing defect and the parameters of the deep drawing process. For example, the effect of blank shape on earing defect (Das et al., 2013; Desai et al., 2005; Nagda et al., 2017; Patel et al., 2015), the effect of tool geometry on earing defect (Gürün & Karaałaç, 2015), the effect of anisotropic nature of blank material on earing defect (Yoon et al., 2017; Trzepieciński & Gelgele, 2010), the effect of temperature on earing defect (Athale et al., 2017; Seo et al., 2018) etc. But the aim of removing earing defect from the final product has been never fully achieved; which means there are other process parameters left which we do not know their effects on earing defect. Hence, the objective of this work is to investigate the relationship between earing defect and varying blank holding force to reduce earing through numerical simulation and experiment. The process setup is attached to a universal testing machine to perform the experiments and for simulations the tools are imported into finite element analysis tool, Pam-stamp 2G, where sheet metal blank was modelled and simulations were carried out. To sum up, Considering the high cost of materials, a reduction in earing defect could bring the manufacturing costs significantly down. Therefore, it is very important to study the earing defect and deep drawing behavior with respect to varying blank holding force using the appropriate experimentation using pre-installed computer-based system on the universal testing machine and numerical simulation.

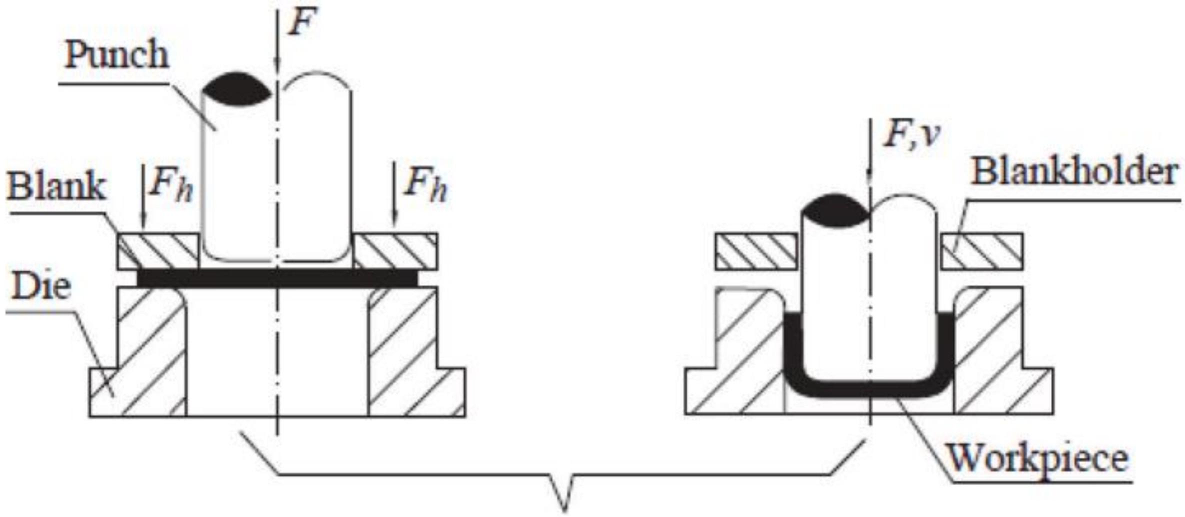

Figure 1.1: Illustration of deep drawing process (Reddy et al., 2016)

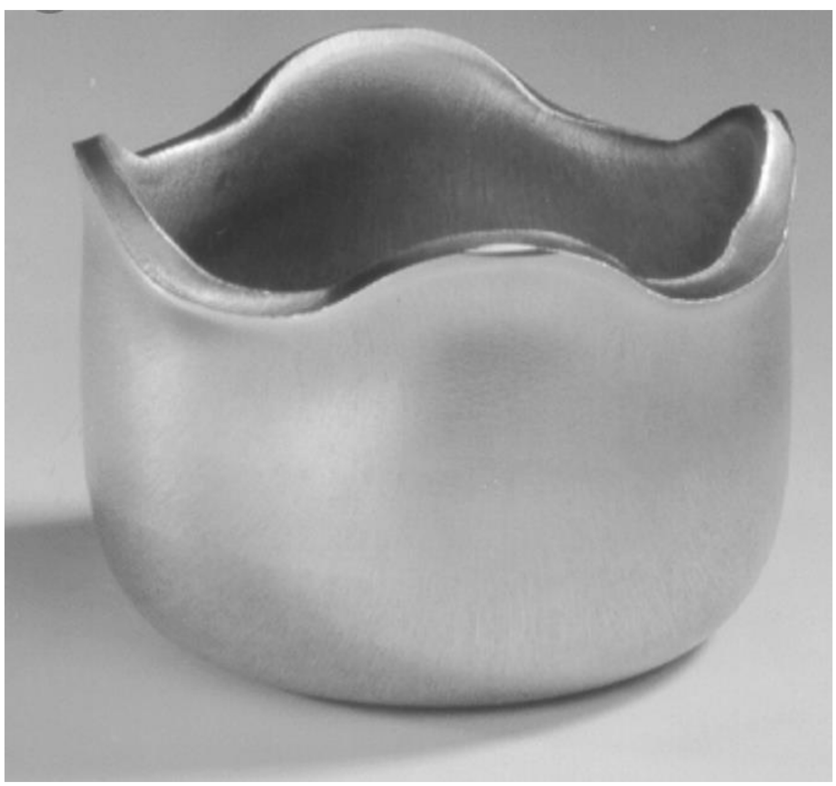

Figure 1.2: Typical appearance of a deep drawn cup with Earing defect (Patel et al., 2015)

1.2 Statement of the problem

Earing is undesirable since it requires an additional processing step where excess metal must be trimmed causing wastage of material and time. Also, the metal representing the ear will be deformed into the cylindrical cup, and this will demand extra load (Nagda et al., 2017).

Earing is one of the major defects observed during deep drawing process (Desai et al., 2005; Patel et al., 2015). it is formation of waviness on uppermost portion of deep drawn cup. Knowledge about ear formation in deep drawing process allows a prior modification of process which can result in defect reduced/ free final product with financial and time saving. Many researches have been performed on the effects of deep drawing process parameters on earing defect. However, it is difficult to find research which explicitly define the effect of blank holding force on earing defect. Therefore, the objective of present study is aimed to investigate the level of the influence that blank holding force have on earing defect and explain what kind of effect it has.

1.3 Objectives

1.3.1 General objective

- The main objective of this thesis is to investigate the influence of blank holding force on earing defect during deep drawing process through finite element analysis and experimentation of AA6061 and Low-carbon steel sheet materials.

1.3.2 Specific objective

- To design the optimized blank size.
- To test the mechanical properties of the material using universal testing machine
- To simulate deep drawing process using Pam-Stamp 2G Finite element software.
- To design and manufacture the die, punch, and blank holder for deep drawing process.
- To experiment on deep drawing process using custom made deep drawing setups.
- To compare the simulation and experimental results.
- To describe what kind of influence does the blank holder force have on earing defect and draw conclusions.

1.4 Significance of the study

Earing defect appears easily during deep drawing of cylindrical parts. There are other causes for the formation of ears during deep drawing process. Some of those causes were studied by other researchers with respect to earing defect. This paper has provided simulated and experimental results of the effects of blank holding force on earing defect. Therefore, this paper will be an input for further researches in deep drawing areas.

1.5 Scope of the study

This thesis work is delimited to numerical simulation and experimentation of AA6061 and low carbon steel sheet metal samples with blank holding force. All other parameters are maintained at constant value except the blank holding force. Testing of the AA6061 and low carbon steel samples with custom made deep drawing tools and available testing facilities and investigates the effect of blank holding force on earing defect.

1.6 Research question

- ✓ What is the influence of blank holding force on earing defect?
- ✓ How much the blank holding force affect the earing profile?
- ✓ What is the optimum blank holding force to have reduced earing height?
- ✓ What are the percentage of earing with respect to different blank holding force?

1.7 Limitation of the study

Limitations during preparation of tensile specimens

- Non- availability of correct sheet metal cutting tools/machines
    - ✓ Due to this limitation, the surface finish along the thickness direction were not good and dimensional accuracy is reduced.

Limitations during tensile and plastic strain ratio testing

- The gripping force of the available tensile and plastic strain ratio testing machine was not good enough to hold any of the specimens.

Limitations during machining of deep drawing tools

- Machining corner radius/ fillet was difficult due to non-availability of fillet making forming tools.
    - ✓ Even though custom made fillet making forming tool was designed and manufactured and sand paper was used to polish the corner radius

surfaces of both punch and die tools, the problem of high surface roughness was observed during the operation. The picture of the fillet making tool can be seen on the appendix D.

- Non- availability of dynamometer
    - ✓ Due to this limitation, reading or applying the correct value of blank holder force was challenging. To reduce the effect of non – availability of dynamometer, spring system was used.
    - ✓ Finding new spring on the market was difficult and for this reason available springs were used during the experiment.

Limitations during circular blank preparation

- Non availability of correct circular blanking tool/machine
    - ✓ Due to this limitation, the surfaces in the thickness direction are not well finished.

1.8 Organization of the thesis

This thesis is organized into five chapters. Chapter one is an Introduction which comprises background of the study, statement of the problem, objectives, and scopes, significant of the study, research questions, limitation, and organization of the thesis. Chapter two presents a review of literatures related with the study that emphasize on study of the effect of blank holding force on earing defect during deep drawing process. Chapter three describes the Materials and Methods used to complete this work. It includes design and preparation of optimum blank size materials and, tensile and plastic strain ratio specimens, and conducting tensile and deep drawing experiments and simulating the deep drawing process. Also, describes some of the basic materials that are used on this study. The fourth chapter focus on results and discussions of the study. The fifth and the last chapter present the conclusion, recommendation and future work respectively.

Chapter Two

2. Literature review

2.1 Introduction

Deep drawing is one of the widely used sheet metal forming process due to its ability to form variety of shapes such as auto body parts, kitchen wear to aerospace parts. Various defects occur during deep drawing operation such as wrinkling, tearing, local necking, earing, fracture, etc. Due to variation of different deep drawing process parameters, earing problem takes place in the plane of sheet. It accounts for maximum amount of material wastage through trimming (Das et al., 2013) and also sometimes edge cracking can take place due to excessive thickening at the rim of cup. There is a need to reduce the earing behavior through some means. Many studies have been performed to explain the relationships between earing defect and some other process parameters of the deep drawing process.

Stages in deep drawing:

1) As the punch pushes the sheet, it is subjected to a bending operation. Bending of sheet occurs over the punch corner and die corner. The outside perimeter of the blank moves slightly inwards toward the cup center. The clearance ‘c’ is defined to equal to 10% more than the sheet thickness ‘t’. If the clearance between the die and the punch is less than the sheet thickness, then ironing occurs.

2) In this stage, the sheet region that was bent over the die corner will be straightened in the clearance region at this stage, so that it will become cup wall region. In order to compensate the presence of sheet in cup wall, more metal will be pulled from the sheet edge, i.e., more metal moves into the die opening.

3) Friction between the sheet and the die, blank holder surfaces restrict the movement of sheet into the die opening. The blank holding force also influences the movement. Lubricants or drawing compounds are generally used to reduce friction forces.

4) Other than friction, compression occurs at the edge of the sheet. Since the perimeter is reduced, the sheet is squeezed into the die opening. Because volume remains constant, with reduction in perimeter, thickening occurs at the edge. In thin sheets, this is reflected in the

form of wrinkling. This also occurs in case of low blank holding force. If BHF very small, wrinkling occurs. If it is high, it prevents the sheet from flowing properly toward the die hole, resulting in stretching and tearing of sheet.

5) The final cup part will have some thinning in side wall.

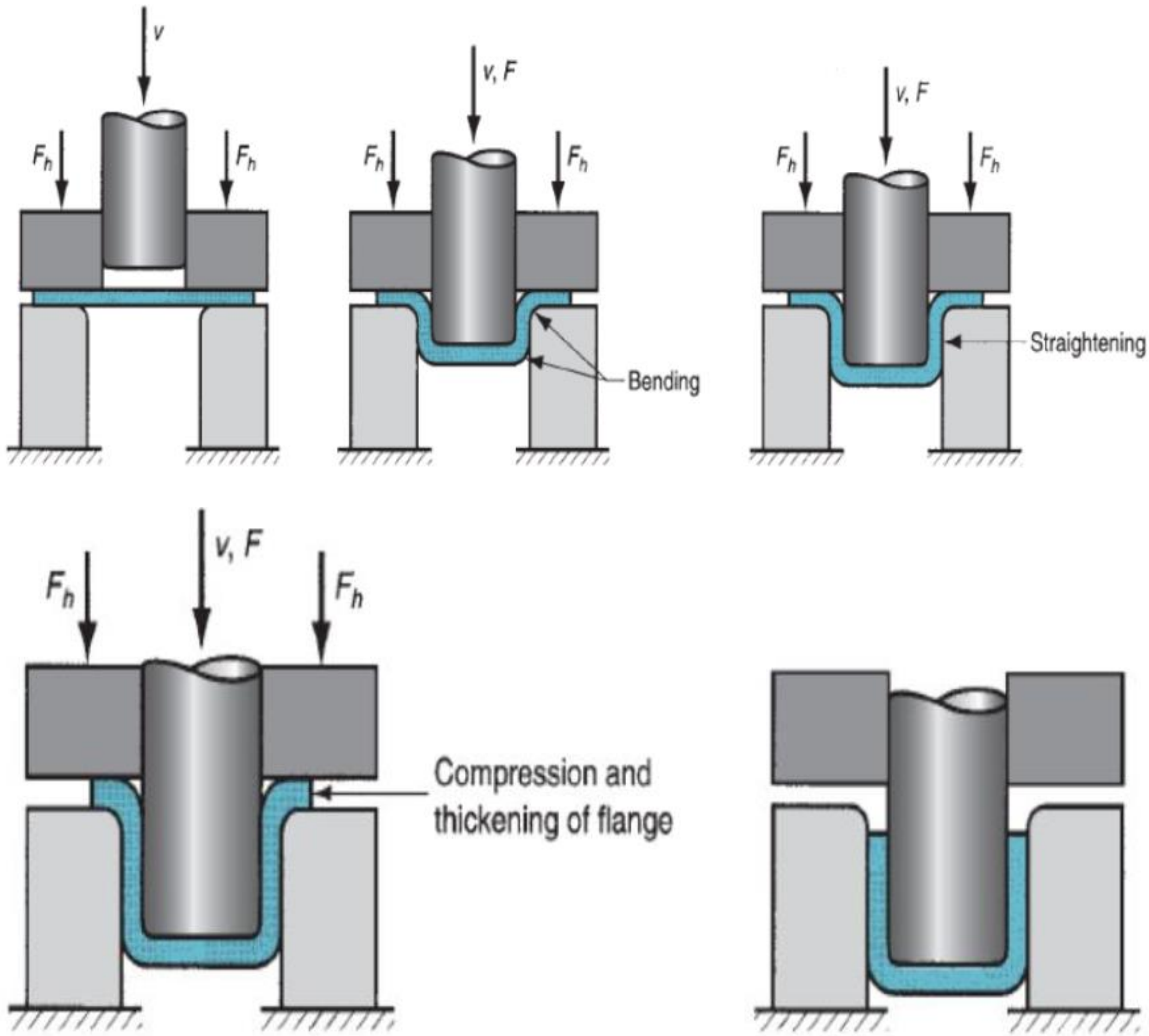

Figure 2. 1: Stages in cup deep drawing operation (Groover, 2010)

2.2 Failures in sheet metal forming operations

There are potential formability problems typically associated with each forming operation. The major problems are earing, fracture, buckling and wrinkling, shape distortion, and undesirable surface textures (Adams et al., 2018; Khairnar et al., 2018). It is important to recognize and understand which defects are associated with a given process and their effects on the finished product.

2.3 Modification of the geometry of the blank

In recent times, few researchers have adopted different approaches and carried out study on minimizing the earing by modifying the initial blank size. Pawan S. et al. (2017) studied deep drawing process with the help of software (ABAQUS) to study cup forming process using EDD steel as blank material. Based on the result they concluded that minimization in the earing defect of deep drawing is possible by modification of initial blank shape. Simulated results showed the initial blank as circular blank produced more % earing height because of planar anisotropy and modified blank showed reduction in the % earing height. The use of modified blank; i.e., non-circular blank produced considerable reduction in % earing height. Ravikant Patel et al. (2015**)** modified initial blank by using non – circular blank shape of low carbon steel. Similar work was carried out by Das et al. (2013) studied the earing problem in deep drawing of cylindrical cups by finite element modeling using HYPERWORKS-6., and modified initial blank shape for IF steel. Both researchers observed significant reduction in earing. Kariem M. Younis and Adil Sh. Jaber. **(2018**) investigated the effect of parameters of the process utilized in square deep drawing process such as; material properties, blank size, blank shape on the height and shape of earing defect appearance of the drawn cup. The results show that, the circular blank give the best results according to earing defect and useful height of the drawn cup, when square shape of blanks were utilized, excessive earing will show in the square cup, due to non-uniform distribution of blank material around the perimeter of the die cavity, minimum material in the flat side and too much material found in the die corner, while when using octagonal shape of blanks which have a same surface area to the square blank, the earing will reduce in the corner of the cup due to extract of the too much material from the blank corners.

2.4 Material properties

The orientation of grains produced by the metal forming process is the primary cause of anisotropy in material. Earing is dependent upon the anisotropic property of material which is generated due to preferred crystallographic texture developed during rolling of sheet (Nagda et al., 2017).

2.4.1 Crystallographic texture

Texture provides a source of directionality because the crystal structures of metals are themselves frequently anisotropic, and then some of this behavior becomes inherited by the material as a whole. Only in the case of a totally random texture do the effects of orientation cancel out completely (Hutchinson, 2015). The development of crystallographic texture during the deep drawing process results in the formation of pronounced plastic anisotropy, including the well-known earing phenomenon (Engler et al., 2019).

Hutchinson, (2015) studied and analyzed the earing profile of single crystal and polycrystal of AA3104 sheet and the potential influence of the initial texture and its spatial distribution on the earing type. The result shows the initial texture and its grain spatial distribution are the major factors determining the earing of AA4104-H19 sheet. Engler et al., (2020) presents a paper that track the evolution of texture, microstructure and earing properties in Al alloy AA 8011A closure stock during downstream processing to final-gauge sheet in temper H14 and the resulting earing properties were discussed in the light of the interplay of deformation and recrystallization with the resultant texture changes along the process chain. Magnesium alloys develop pronounced crystallographic texture and plastic anisotropy during rolling, which leads to earing during deep drawing of the rolled sheets and study (Ohwue & Kobayashi, 2014) shows the predicted earing pattern is found to depend not only on the initial texture at the beginning of the drawing process, but to a large extent also on the evolution of texture during drawing.

2.4.2 Anisotropy

Anisotropy, sometimes also referred to as directionality (Hutchinson, 2015), is a very commonly observed phenomenon whereby properties of a material vary, depending on the direction along which they are measured. The converse of anisotropy is, of course, isotropy where the material shows equal properties in all directions of measurement. True isotropy is a remarkably rare thing in ordinary materials and is actually quite difficult to achieve. Directionality arises out of most kinds of material processing including consolidation and plastic working, so it is seldom avoided.

If the magnitude of the planar anisotropy parameter, ΔR, is large, either, positive or negative, the orientation of the sheet with respect to the die or the part to be formed will be important; in circular parts, asymmetric forming and earing will be observed. If the normal anisotropy ratio R is greater than unity it indicates that in the tensile test the width strain is greater than the thickness strain; this may be associated with a greater strength in the through-thickness direction and, generally, a resistance to thinning. Normal anisotropy R also has subtler effects. In drawing deep parts, a high value of R allows deeper parts to be drawn. In shallow, smoothly-contoured parts such as auto body outer panels, a higher value of R may reduce the chance of wrinkling or ripples in the part. Other factors such as inclusions, surface topography, or fracture properties may also vary with orientation; these would not be indicated by the R- value which is determined from plastic properties (Wang et al., 2019).

The microstructure of metallic materials can be either isotropic or anisotropic. This means that the microstructure can be either constant in all directions or be aligned in a certain direction. If the metal has any pattern or alignment of its microstructure, it is said to be anisotropic. Anisotropy is considered in two forms; normal and planar. Normal anisotropy measures the change in material characteristics, which differ through the thickness of the sheet, while planar anisotropy measures material characteristic differences in various directions within the plane of the sheet. Fig. 2.1 defines normal and planar anisotropy relative to the sheet (Groover, 2010). The microstructure of the metal can have great impact on the ability of the metal to be formed into the desired shape. A prevalent cause for planar anisotropy in sheet metals is the rolling direction. During processing of sheet metal, the rolling operation elongates and aligns the grains of the metal's microstructure in the rolling direction and packs the grains in the thickness direction, which leads to significantly different strength properties within the material. During a tensile test, the width of the material and the thickness decrease as the elongation increases. The plastic strain ratio, r, is the ratio of width strain to thickness strain. The ratio is useful for determining the degree of anisotropy in the material and rating its resistance to thinning. If the ratio is equal to one, then the material is isotropic, since the strain is equal in both thickness and width. The r ratio values are a measure of the drawability of the sheet metal (Groover, 2010). For high strain ratios, the material is said to be resistant to thinning, while materials with low strain ratios will be undesirable for forming operations, since it will thin and possibly rupture.

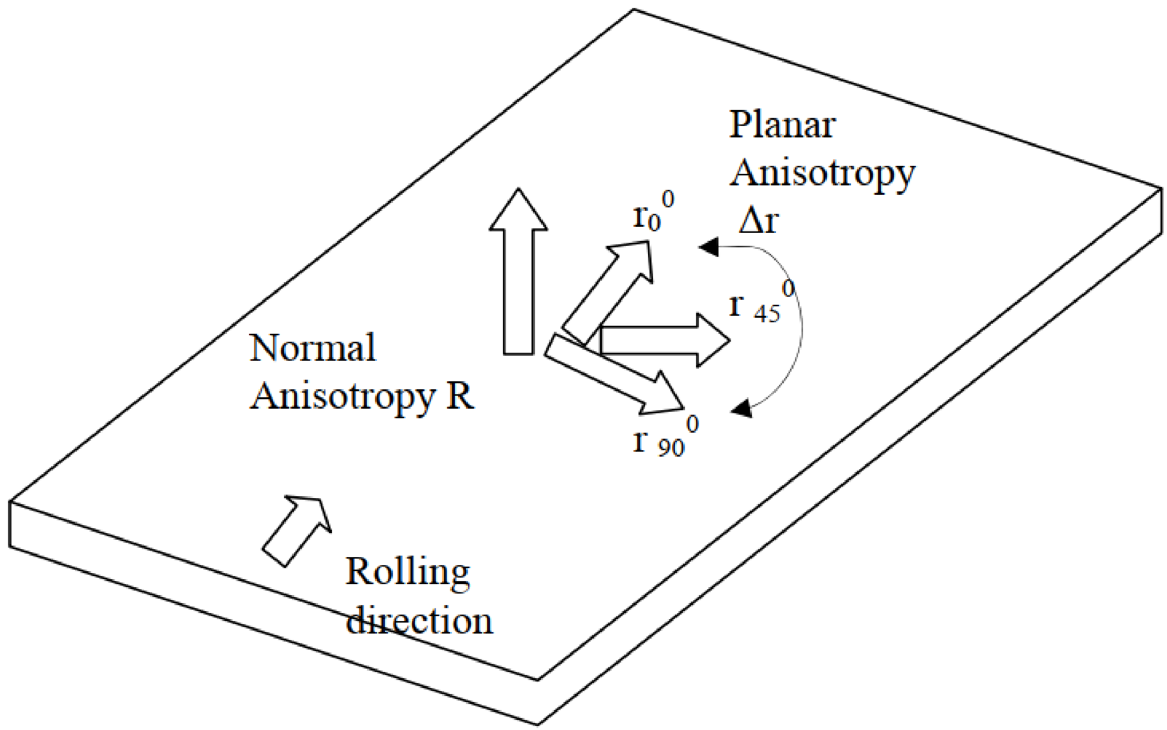

Figure 2. 2: Sheet orientation relative to normal and planar anisotropy (Groover, 2010).

The strain ratio is determined relative to the rolling direction of the sheet material, thus r_0 (parallel), r_{45} (diagonal) and r_{90} (transverse) can be determined through geometry. The plastic anisotropy coefficients are assessed by the means of plastic strain ratios of these three planes which are also called as Lankford coefficients. The weighted average, R, of these strain ratios, which is also called normal anisotropy. The Earing tendency is simply the likelihood that the sheet will draw non uniformly and form ears in the flange (Groover, 2010).

2.5 Geometry of deep drawing tools

O. O. Oluwole1 **et al. (2010)** studied the effect of blank/punch diameter ratio (draw ratio) in deep drawing on earing for different gauges of Al 1200 sheet draw cups; and the result showed that earing was observed to generally increase with increasing draw ratio using the same sheet thickness. It was also observed that for thinner sheets (0.6-0.9mm), using the same draw ratio, earing increased with increasing sheet thickness. For thicker sheets (1.2-1.58mm) earing was observed to decrease with increasing sheet thickness. After that, there was an increase for deep-drawn 2mm thick sheet; and higher draw ratios were observed to draw deeper cup depths with minimal earing. FE simulation of earing shape in deep drawing process is studied by Saxena and

Dixit (2009). In this study the geometry of tool and parameters of process on the formation of ears was investigated. It was found the ultimate ear height in a cylinder cup are influenced by the anisotropy nature of material, moreover the earing reduces with increase in the radius of the die and punch profile.

2.6 Blank holding force

Blank holder force is one of important factors to control the drawing process. To avoid fracture and wrinkling, numerous researches have been done numerically and experimentally, to obtain optimum variable blank holder force trajectory or to control blank holder force region by region (Srirat et al., 2012)**.** Even simplest drawing operation, the thickness of the work metal and die radius offers some restraint to the flow of the metal into the die. For drawing all but simplest of the shape some restraint is required for the controlling the flow of the material. However, during the forming stage, the blank holder does not make contact with the entire blank which means that it cannot fully control the material flow (Ohwue & Kobayashi, 2014). Moreover, when a higher restraining force is needed, higher blank holder force must be applied. To reduce the flow of material between the binder faces or increase restraining force, it is not good practice to simply keep increasing the blank holder force. This results in higher stress values being imposed on the die and press which may cause excessive wear in the tools and galling in the blank

Compressive forces on the metal in the area beyond the edges of the die cause the work metal to buckle. If this buckled or wrinkled metal is pulled into the die during the drawing operation, it increases the strain in the area of the punch nose to the point at which the work metal would fracture soon after the beginning of the draw. The blank holder force is used to prevent this buckling and subsequent failure. The amount of blank holding force required is one third of the drawing (Groover, 2010). As we can say that blank holding force prevent blank from the buckling and for the proper distribution of the strain, blank holding force is required otherwise problem like wrinkles can also occur with or without friction. Han et al (2013). investigated optimum drawing process by changing circumferentially the blank holder forces, to draw earless circular cups from anisotropic blank sheet and the result shows distributing the blank holding force region by region gives the best result in reducing the height of the earing defect when compared to uniformly distributed force. However, the conclusion derived from this study is not clear enough to grasp the effect and mostly depend on the analytical analysis. Generally, the material flow is controlled by the blankholder: a restraining force is created by friction between the tools and the blank. As a result, the tensile stresses are increased, material flow is controlled, and the formation of wrinkles is avoided. Blank holder force plays a major factor in the formability of sheet metals. If the blank holder force is too low, then wrinkling in the flange or the wall will occur. If the blank holder force is too high, then excessive thinning or fracture occurs.

2.7 Process parameters

Process parameters are the variables that affect directly to the formability characteristics. In the try-out stage, one of these parameters are changed slightly while the other kept constant until desired geometry obtained. after the accurate parameters which is the blank holding force was figured out then the deep drawing process is processed.

2.7.1 Mesh density

The basic idea of finite element analysis (FEA) is to make calculations at only limited (Finite) number of points and then interpolate the results for the entire domain (surface or volume). Any continuous object has infinite degrees of freedom and it’s just not possible to solve the problem in this format. Finite Element Method reduces the degrees of freedom from infinite to finite with the help of discretization or meshing (nodes and elements).

In finite element analysis (FEA), the accuracy of the FEA results and requested computing time are determined by the finite element size which provides mesh density(Yalçın, 2010). According to FEA theory, the FE models with fine mesh (small element size) yield to highly accurate results but may take longer computing time. On the contrary, those FE models with coarse mesh (large element size) may lead to less accurate results but do save more computing time. Also, small element size will increase the FE model's complexity which is only used when high accuracy is required. Large element size, however, will reduce the FE model's size and is extensively used in simplified models in order for providing a quick and rough estimation of designs. Due to its importance, in generating FEA models, the foremost problem is to choose appropriate elements size so that the created models will yield accurate FEA results while save as much computing time as possible. In the current paper, mesh size of two is used for the blank materials and rigid mesh is used for the die, punch and blank holder as it is applied in (Patel et al., 2015).

2.7.2 Punch Speed

Caglar, (2005) studied the effects of punch speed on the quality of the product of steel and aluminum with thickness of one (mm) and found that increasing the speed will reduce the time required for the simulation process and it has no direct effect on the qualities of the product. This study also incorporates the effects of blank holder force considering the punch speed and the result is if the blank holder force is increased thoroughly, the tendency of the blank material for failure will increase dramatically. The speed of the punch is taken as 1mm/sec as it is given by Caglar, (2005).

2.7.3 Friction Coefficient

Friction, as expressed by the value of the coefficient of friction (CoF), also affects the potential failure of the drawn cup. When the friction between the drawn part and the punch is low, then failures will occur in the base of the part. If the friction between the part and the punch is high, the base of drawn part will be increasingly stressed with increasing friction in the can body so that the failure zone will be moved to the body of the drawn can (Lăzărescu & Banabic, 2017). CoF depends on the selected lubricant, surface conditions and the blank holder pressure on the flange. In cup drawing, the blank holder controls the flow of material into the die and reduces the formation of wrinkles in the flange. However, because of the friction between the blank holder and the sheet in the flange area, the blank holder force affects friction and metal flow. Therefore, an optimum blank holder force must be determined for each drawing operation based on the sheet material, thickness, and testing conditions to keep the friction shear stress in the flange area as low as possible while preventing wrinkle formation (Fallahiarezoodar et al., 2014).

2.7.4 Limiting Drawing Ratio

Limiting drawing ratio represents the largest blank that can be drawn through a die without tearing and wrinkling (D.Younis, 2010). It has been found that when the blank size exceeds a critical diameter, buckling at the flange and higher stretching at punch corner does not allow sufficient material flows into the die cavity which leads to necking and failure (Oluwole1* et al., 2010). During an LDR test, successful drawing implies that there is no necking or wrinkling in the drawn cup, which has no flange at the end of the process (Fallahiarezoodar et al., 2014).

2.8 literature summary and research gaps

- The reviewed literatures demonstrated that deep drawing process parameters could affect earing defect and solutions were given to solve the problem in related to specific process parameter. However, the previous researches mainly focus on the effects of process parameters on earing defect other than blank holding force and the effect of blank holding force with related to earing defect wasn't investigated explicitly. Hence this thesis will fill the void of such limitation on the relationship between varying blank holding force and earing defect.
- Deep drawing process parameters which have a relationship with earing defect have been studied independently with different scholars. But the study was limited to those parameters other than blank holding force and it wasn't investigated explicitly. Hence, this thesis will fill the void of such limitation and on the effect of varying blank holding force on earing defect.

2.9 Application

AA6061 alloy and Low – Carbon steel sheets still are most commonly used in the aerospace, automotive, water treatment, power storage, battery, electrical, plumbing, thermal and pharmaceuticals industry. Their components are preferred because of their excellent strength to weight ratio, ability to harden after deformation, resistance to corrosion, light-weight, recyclable, ductility, thermal conductivity and excellent formability (Han et al., 2013; Patel et al., 2015).

Some of the components produced using the above materials are:- Cans, caps, cases, collars, components, connectors, couplings, cups, enclosures, eyelets, ferrules, fittings, hubs, housings, sensors, shells, sleeves, tubes(Han et al., 2013).

Chapter 3

3. Materials and Methodology

3.1 Material selection

The material selected in present study is aluminum, low carbon steel sheet metals with 1mm thickness. These materials have been selected based on extensive use in today's life, the market availability and mechanical properties. Further, they have good drawability, bywhich better formabilty is expected. These qualities permit successful forming, deep drawing, bending, etc.

3.2 Starting stock

The size and shape of the blank are important for material consumption, for the design of the deep drawing tooling and the cost-effectiveness of the process. When determining the size of the blank, it is assumed that the material thickness remains constant throughout drawing.

The first step in designing the drawing setup is to design or decide the geometry and size of the blank material. Most of the cases, either circular blank or rectangular blanks are used. A better earing results were observed by using circular blank from the literatures (Das et al., 2013; Desai et al., 2005; Dixit, 2009; Nagda et al., 2017; Patel et al., 2015). So, in this thesis, circular blank was selected. To determine the size of the blank and the steps of deep drawing, the following three rules (Groover, 2010) were considered: -

1) The maximum limiting draw ratio should be less than two.

Limiting draw ratio, $\mathrm{LDR} = \frac{\mathrm{D}}{\mathrm{d}} \leq 2$ …………………………………………………………….. (3.1)

2) The reduction should be less than 0.5.

Reduction, $\mathrm{R} = \frac{\mathrm{D-d}}{\mathrm{D}} < 0.5$ ……………………………………………………………… (3.2)

3) The thickness to cup diameter ratio should be greater than 1%.

$\frac{\mathrm{t}}{\mathrm{D}} > 1\%$ ………………………………………………………………(3.3)

If the above three rules are fulfilled, then the part can be produced in one draw.

Determining the blank size for cylindrical parts using equation 3.4 with small radii (r < 10 mm)

Cup without flange shown in the Fig. 3.1.

$$D = \sqrt{d^2 + 4dh} \quad \ldots\ldots\ldots\ldots\ldots\ldots\ldots\ldots\ldots\ldots\ldots\ldots\ldots\ldots\ldots\ldots\ldots\ldots\ldots\ldots\ldots\ldots\ldots\ldots(3.4)$$

where D – diameter of the blank

d – diameter of the cup

h – height of the cup

In this paper, the drawing step is selected to be one considering the cost of drawing tool materials.

Blank holder is not required if the height of deep drawn cup is five times the thickness (h = 5t) of the starting blank material (Groover, 2010). In this paper, blank holder is used since the selected height of the cup is greater than 5t.

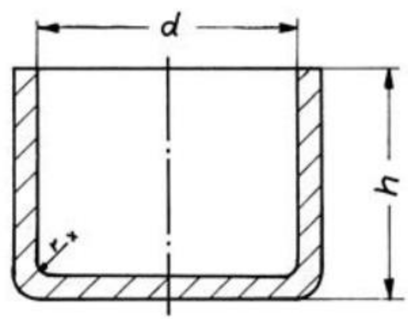

Figure 3. 1: Cup with small bottom radius (r < 10mm)

At first, the diameter of the punch is taken as 48mm randomly and select the height of the cup which is greater than 5t. Then the diameter of the initial blank is calculated by inserting different values of height. Finally, verify whether the calculated blank diameter fits the design rule; if not, change the height of cup and follow the same procedure.

$$D = \sqrt{48^2 + 4(48)(30)} = 89.8 \approx 90\text{mm}$$

Limiting draw ratio, LDR $= \frac{D}{d} \leq 2$

$$\text{LDR} = \frac{90}{48} \leq 2$$

$$LDR = 1.87 \leq 2$$

Reduction, $R = \frac{D-d}{D} < 0.5$

$$R = \frac{90-48}{90} < 0.5$$

$$R = 0.465 < 0.5$$

Thickness to diameter, $\frac{t}{D} > 1\%$

$$\frac{1}{90} > 1\%$$

$$1.1\% > 1\%$$

Therefore, the part can be produced in one draw.

The clearance between the die and cup is calculated based on (Groover, 2010) using equation 3.5 and thickness of the sheet metal is taken as 1mm.

$$c = 1.1t \quad \text{………………………………………………………………….(3.5)}$$

$$= 1.1 * 1$$

$$= 1.1\text{mm}$$

Based on the above rules and methods, there are other blank diameter values which fulfill the above procedure such as 78mm with height of cup 20mm, 84mm with height of cup 25mm, and 90mm (the maximum diameter based on the flange area of the die) with height of cup 35mm (the maximum height which fits the design rule considering one step drawing operation). The deep drawing tools used in this work were designed by selecting 90mm diameter of the initial blank size.

3.3 Design of deep drawing tools

Considering the above value of blank diameter (D = 90mm), the draw setups were designed using Solidworks 2021. The design of punch, die, blank holder and assembly of deep drawing process as per the blank size shown in fig. 3.2 to fig. 3.5. The dimensions of each part also represented in the respective Figures.

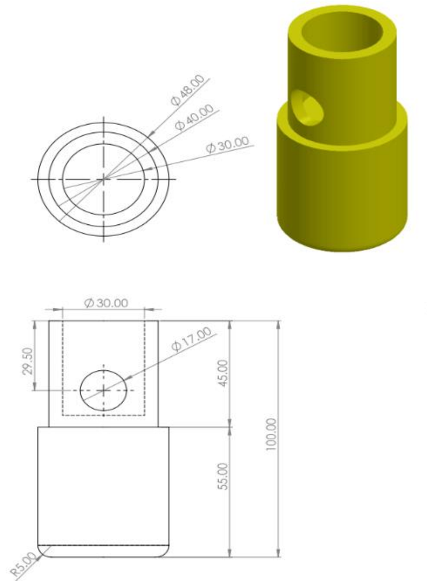

Figure 3. 2: CAD model of Punch

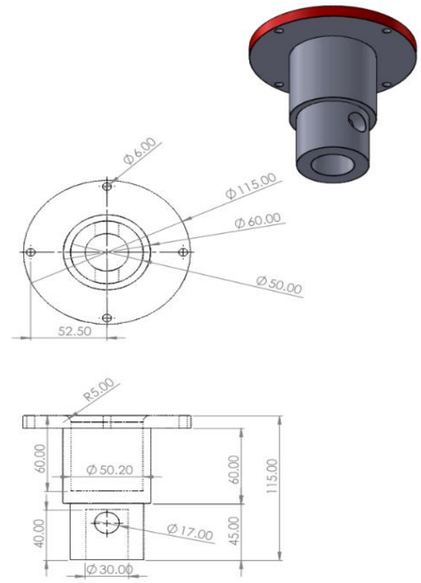

Figure 3. 3: CAD model of Die

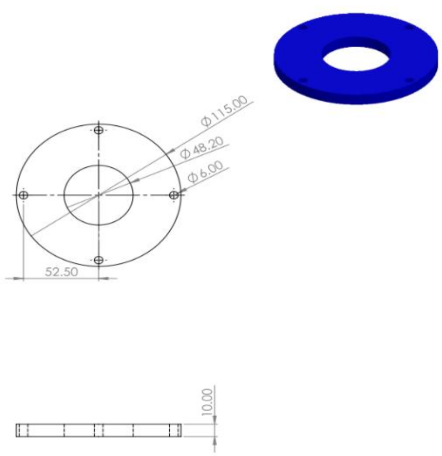

Figure 3. 4: CAD model of Blank holder

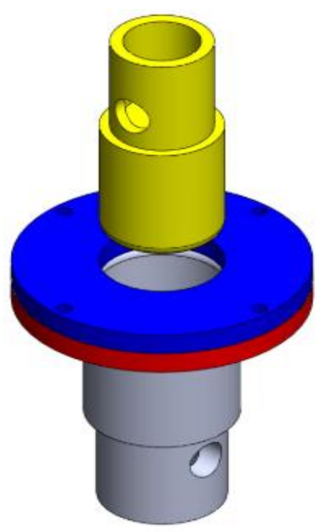
Figure 3. 5: CAD model of Assembly

3.4 Preparation of tensile specimens

To define the properties of the sheet metal (blank), specimens were designed and prepared according to ISO (International Standard Organization) standard ISO 6892-1 2016 specification as shown in Fig. 3.6. The dogbone and rectangular shape Specimens were prepared from AA6061 alloy and Low- Carbon steel metal sheets at different orientations with respect to the rolling direction: 0°, 45° and 90°; and for each rolling direction, three specimens were prepared for tensile testing and one for plastic strain ratio testing.

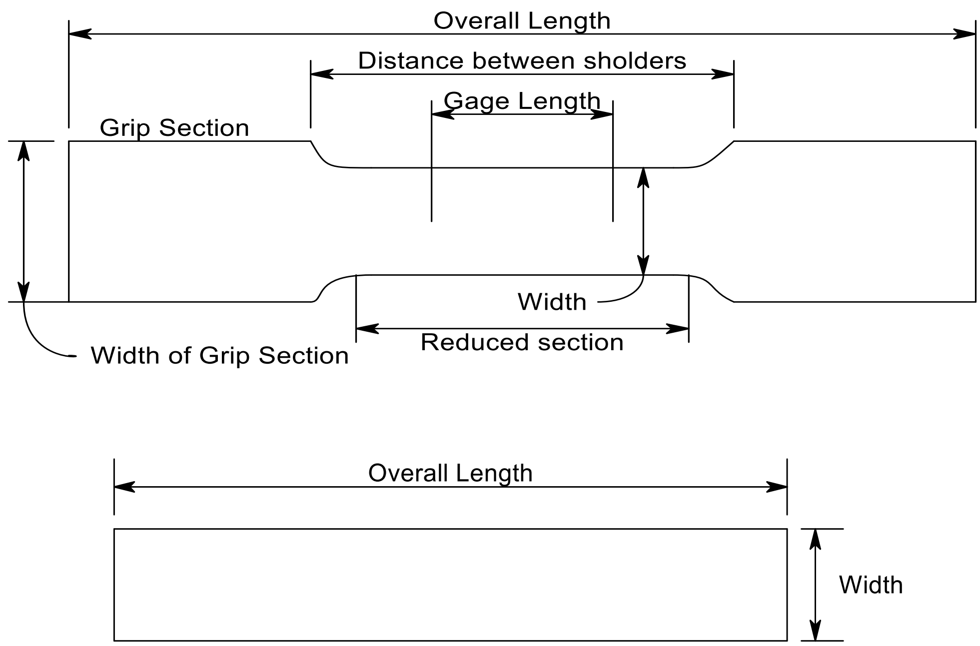

Figure 3. 6: Schematic representation of tensile and plastic strain ratio test specimen according to (ISO 6892-1 2016 specification)

3.5 Uni-axial Tensile test

To evaluate the mechanical properties of the sheet metal (blank), the tensile specimens were tested, with the direction of rolling (0^o), diagonal (45^o), and perpendicular (90^o). All pre-fabricated specimens were tested at cross head speed of 2mm/min, using universal testing machine (UTM) with model WP 310 by custom made specimen grippers. The standard tensile specimens were tested until fracture occurred and the standard plastic strain ratio specimens were tested up to their 10% elongation. The specimens were suitably mounted on a calibrated UTM with proper alignment and sufficient gripping force as shown in Fig. 3.7.

The top gripper moves with a constant crosshead speed which continues till failure of the specimen. The amount of load applied to the specimens and their corresponding elongation were measured throughout the testing process and plotted on a stress strain curve until fracture. Measurements like UTS, yield strength, and initiation of necking were calculated. The broken samples were placed back together to measure their length just before failure and measured maximum strain obtained via comparison with their original lengths.

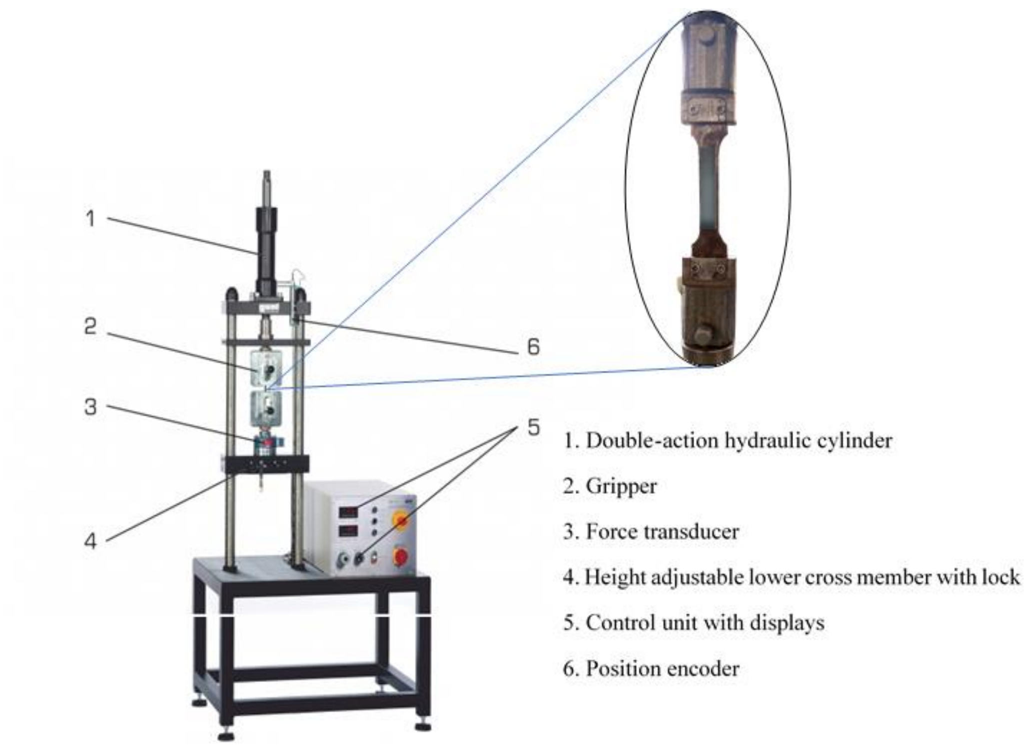

Figure 3. 7: Hydraulic Universal Material Tester, 50kN

3.5.1 Stress- Strains plots for mechanical properties evaluation

Stress-strain curve for material is plotted by elongating the sample and recording the stress variation with strain until the sample fractures. It is often assumed that the cross-section area of the material does not change during the whole deformation process. This is not true since the actual area decreases while deforming due to elastic and plastic deformation. So, true stress-true stain values evaluated using instantaneous area.

Engineering stress is calculated (Groover, 2010) by:

$$\sigma = \frac{F}{A} \quad \text{……………………………………………………………………………..(3.6)}$$

Engineering strain is calculated by:

$$\varepsilon = \frac{\Delta l}{l_0} \quad \ldots\ldots\ldots\ldots\ldots\ldots\ldots\ldots\ldots\ldots\ldots\ldots\ldots\ldots\ldots\ldots\ldots\ldots\ldots\ldots\ldots\ldots\ldots\ldots\ldots..(3.7)$$

Where F- Load in (N)

A- Cross-sectional area of specimen before deformation has taken place

Δl- change in length

l_0- Original value of the gage length

True stress is the stress determined by the instantaneous load acting on the instantaneous cross-sectional area.

$$\sigma_t = \sigma \frac{l}{l_0} = \sigma * (1 + \varepsilon) \quad \ldots\ldots\ldots\ldots\ldots\ldots\ldots\ldots\ldots\ldots\ldots\ldots\ldots\ldots\ldots\ldots\ldots\ldots\ldots\ldots\ldots(3.8)$$

$$\varepsilon_t = \ln(1 + \varepsilon) \quad \ldots\ldots\ldots\ldots\ldots\ldots\ldots\ldots\ldots\ldots\ldots\ldots\ldots\ldots\ldots\ldots\ldots\ldots\ldots\ldots\ldots\ldots\ldots\ldots(3.9)$$

Holloman's equation

For metal deformation, the strain-hardening phenomenon was explained by Holloman power law (Palaparti, 2014) as follows:

$$\sigma = K\varepsilon^n \quad \ldots\ldots\ldots\ldots\ldots\ldots\ldots\ldots\ldots\ldots\ldots\ldots\ldots\ldots\ldots\ldots\ldots\ldots\ldots\ldots\ldots\ldots\ldots\ldots.. \quad (3.10)$$

Where: σ = true stress (MPa)

K = strength coefficient (MPa)

ε = true strain

n = strain hardening exponent

Formability of a sheet metal is subject to its strain hardening exponent (n) value. Larger value of strain hardening exponent (n) corresponds to better formability since those materials can withstand larger deformation prior to initiation of necking.

3.6 Plastic strain ratio (r)

The Plastic Strain Ratio, r is considered a direct measure of sheetmetal drawability and is useful for evaluating materials intended for forming shapes by a deep-drawing process. The r value is calculated from width and longitudinal strain as a test specimen is pulled in tension. Its determination was governed by ASTM E517 standard for plastic strain ratio ‘r’ for sheet metal. The plastic strain ratio ‘r’, is given by

$$r = \frac{\varepsilon_w}{\varepsilon_t} \quad \text{……………………………………………………………………………… ….} \quad (3.11)$$

Where: true width strain (ε_w) = $\ln(w_f / w_0)$,

true longitudinal strain (ε_t) = $\ln(t_f / t_0)$,

w_f = final width,

w_0 = original width,

t_f = final thickness,

t_0 = original thickness.

From equation 3.11, the r-value is dependent on the ratio of width and thickness changes as the sample is pulled in tension. It is very difficult to accurately measure changes in thickness, by assuming the volume of the specimen remains constant and express the longitudinal strain as:

$$r = \frac{\ln\left({W_0}/{W_f}\right)}{\ln\left({L_f W_f}/{L_0 W_0}\right)} \quad \text{………………………………………………………………………} (3.12)$$

Where: L_f = final length; L_0 = original length

Equation 3.12 enables the plastic strain ratio (r) to be calculated manually by measuring the change in axial gage length and the change in width. In this approach, prior to testing the specimen width and distance between gage marks is measured with calipers. The specimen is then pulled to a strain less than at maximum force (before onset of necking) and then unloaded. The final width and gage length are then measured to determine r-value.

Using the r-values in three directions (0°, 45°, and 90° to the rolling direction), two other important parameters also calculated (Esther, 2017). 'Planar anisotropy parameter' (Δr), which is an indicator of the ability of a material to demonstrate a non-earing behavior (lower is better), can be calculated using equation 3.13. 'Normal anisotropy parameter' (r_m), which is an indicator of the ability of a material to be deep drawn (higher is better), can be calculated by equation 3.14.

$$\Delta r = {(r_0 + r_{90} - 2r_{45})}/{2} \quad \ldots\ldots (3.13)$$

$$r_m = {(r_0 + r_{90} + 2r_{45})}/{4} \quad \ldots\ldots (3.14)$$

3.6.1 Plastic strain ratio experimental setup

The samples for plastic strain ratio R-value determination tests were prepared as per ASTM-E517 standards. It is achieved through stretching axially on a UTM. Four symmetrical markings (with a permanent marker) have been applied on the test samples prior to testing as shown fig. 4.4, so that the change in length between these markings are measured after the stretching test.

3.6.2 Experimental procedure

a) Preparation of samples as per the specification and marking dots carefully on their surfaces.

b) Mounting the specimens on the UTM and stretch the specimens up to 10% elongation of the original length.

c) Dismount the specimens and measure the length and width change between the dots.

d) Insert the obtained values in the equation 3.13 and calculate the r-value.

3.7 Finite Element Modeling

Simulation procedures

a) Deep drawing set-ups are modelled with the blank using Solidworks 2021 prior to the simulation
b) The modelled set-ups are imported into Pam-stamp 2G simulation software
c) The parts are assembled and process parameters are assigned
d) Material property is assigned for the blank

e) The blank is meshed with size two and the die, punch and blank holder meshed with rigid mesh.
f) Deep drawing simulation is run
g) The simulated results are discussed

When the cylindrical cup drawing process was modeled for a drawing setup Das et al., (2013) work was considered as shown in fig. 3.8(a). It is seen that die and cylindrical punch having 51.1mm and 48mm diameter respectively. Further, the corner radius on die and punch were 8mm and 6mm respectively. Surface model of deep drawing assembly is in shown in fig. 3.8(b) for numerical simulation.

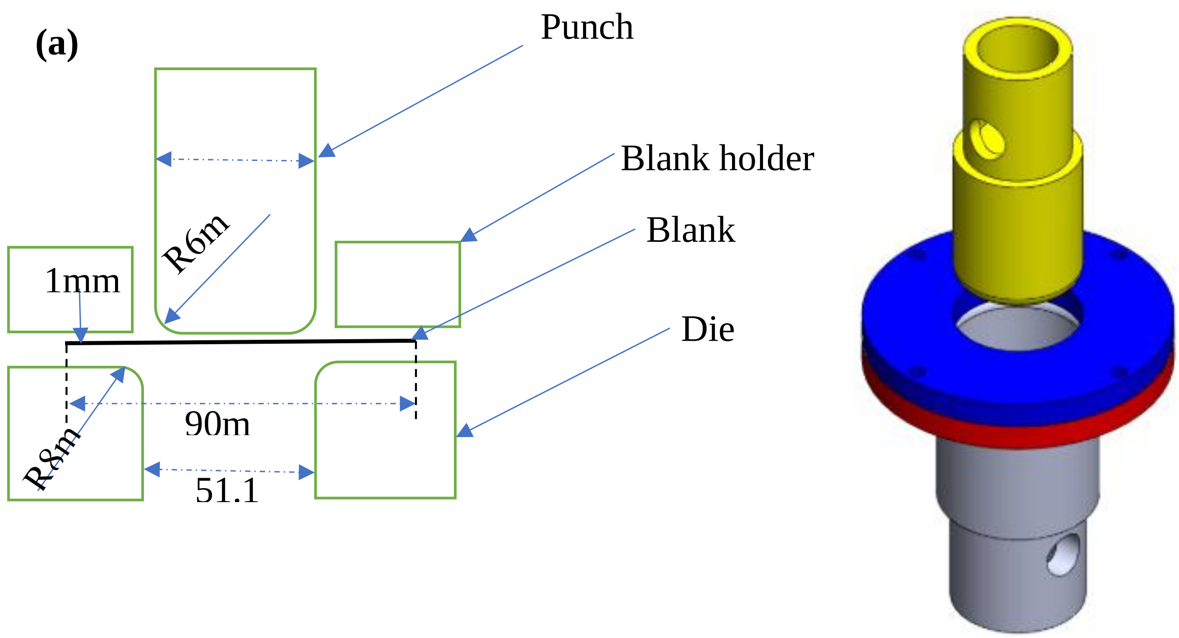

Figure 3. 8: a) schematic illustration and b) Surface model assembly of deep drawing setup for simulation

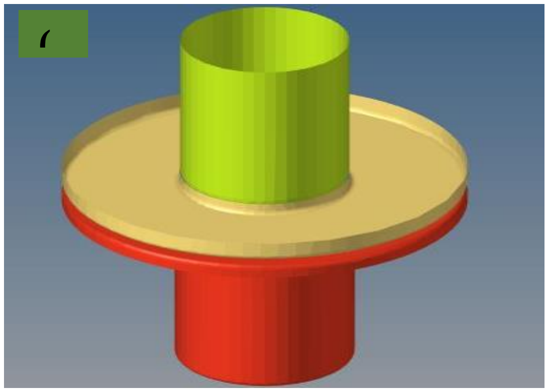

The different boundary conditions were applied into finite element modeling are as indicated in Table 3.1.

Table 3. 1: process parameters

Tool dimensions	Values	
Punch velocity (mm/s)	0.5	
Punch displacement (mm)	50	
Friction between:	Punch and Blank	0.125
	Die and Blank	0.1
	Blank holder and Blank	0.1
Punch diameter (mm)	48	
Punch radius (mm)	6	
Die diameter (mm)	51.1	
Die radius (mm)	8	
Sheet metal thickness (mm)	1	
Initial blank diameter (mm)	90	
Drawing ratio	1.67	
Clearance(mm)	1.1	
Lubricant	Hydraulic oil	

3.8 Cup height and % earing height

The cup heights were measured at different points with respect to width as shown in the fig. 3.9. Variation of cup height is better observed in terms % ear height where % ear height is calculated using eq. (3.15) as given by (Patel et al., 2015) under:

$$\%\ \text{ear height} = \frac{\text{maximum cup height} - \text{minimum cup height}}{\text{minimum cup height}} \times 100 \quad \ldots\ldots\ldots\ldots\ldots\ldots\ldots\ldots\ldots (3.15)$$

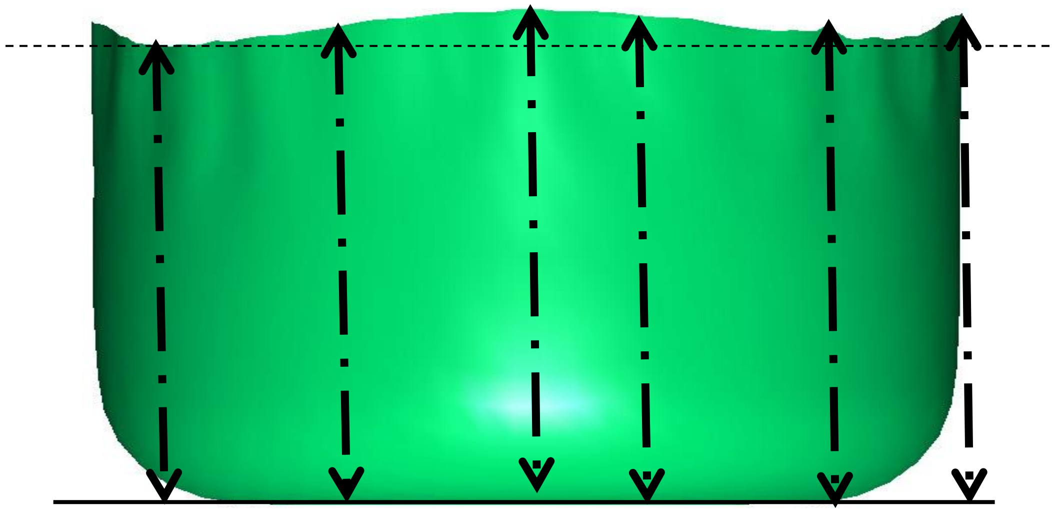

Figure 3. 9: simulated cup showing variation of height

3.9 Deep drawing experimental tooling

The deep drawing of cylindrical cups was carried out by designing and manufacturing custom made deep drawing setup. The deep drawing setup tools were selected by following appropriate tool manufacturing principles. Punch and die were designed and built to produce cylindrical cup, as shown in fig. 3.10. They were made from tool steel, and were machined by manual lathe machine. Then polished to obtain finer surface finish. The rigid cylindrical punch is 48 mm diameter, punch corner radius is 6mm which gives radial clearance of $1.1t_o$ at assembly with the die which has a flat surface with a cylindrical cavity 51.1mm diameter, die corner radius is 8mm.

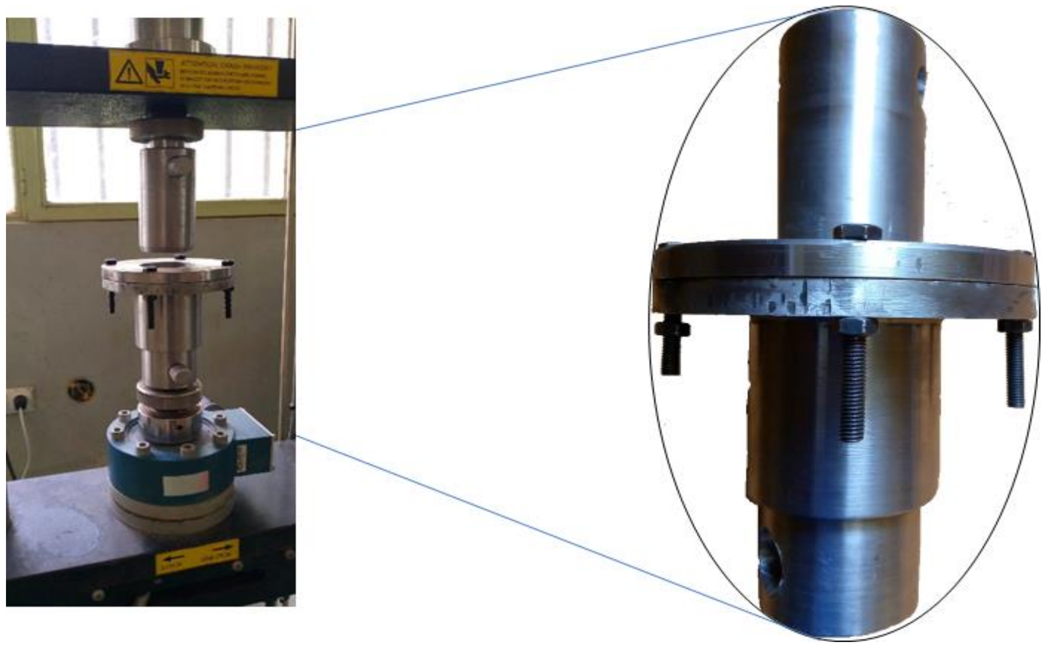

Figure 3. 10: Deep drawing tooling

3.9.1 Deep drawing experimental work

In order to investigate the evolution of the earing defect during the deep-drawing process under different blank holder force conditions (BHF), seven BHF cases were considered. These seven cases of BHF conditions were: 10, 20, 30, 35, 40, 50, and 60kN, respectively. Before starting each individual test, the tools and the blank were cleaned using alcohol, after which lubricant was applied. The lubricants used in experiments were hydraulic oil (HLP 46) which are available on the market.

Deep drawing experiments were carried out to obtain cylindrical cup, where deep drawing die is placed on the tensile testing machine (WP 310). After putting blank on the blank holder surface, taking into consideration the direction of rolling of the sheet (45˚ from RD of the sheet form cup), punch moved towards the die, and this means direct drawing die use. The speed of drawing equal to (60mm/min) was selected to draw for the AA6061 and Low-Carbon steel sheet material. The blank holding force was set as the minimum to prevent defects mainly earing defect by considering prior researches, they were (9kN) for AA6061 alloy and (20kN) for low carbon steel material.

3.10 Circular blank preparation

Circular specimens were prepared for deep drawing by blanking them into 78, 84, 90 and 95mm blank diameters from AA6061 and low carbon steel sheet metals with thickness of 1mm. In this work, 90mm circular blank is selected as shown in the figure below.

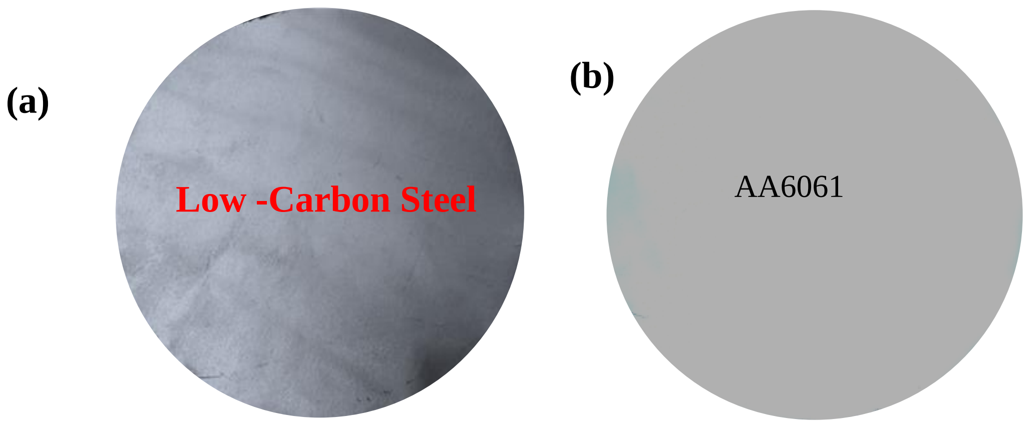

Figure 3. 11: Initial blank with 90mm diameter (a) low carbon steel (b) AA6061 alloy

During the preparation, sheet metal scissor was used to cut out the circular blank and grinder is used to finish the surface in the thickness direction.

Chapter 4

4. Results and Discussion

This section is describing about the experimental studies that are performed. The aim of this study was to understand the effect of blank holding force in earing problem. In order to study blank holding force effect, two different sheets materials, AA6061 and Low carbon steel sheets with 1mm thickness are used. In order to obtain the mechanical properties of these materials, tensile test is performed. After obtaining the material properties, deep drawing experiment is conducted. The materials used in for this work are Al 6061 alloy and low carbon steel. The chemical compositions of Al 6061 alloy and low carbon steel were performed at Adama steel factory and are shown in Table 4.1.

Table 4. 1: Chemical compositions of AA6061 and low carbon steel

materials \ elements	Al	Mg	Si	Fe	Cu	Cr	Zn	Ti	Mn	K	C	others
AA6061	96.8	0.9	0.7	0.6	0.3	0.25	0.2	0.1	0.05			0.05
Low carbon steel			0.28	98					1.03	0.04	0.25	

4.1. Tensile test

In order to find the mechanical properties, tensile tests were conducted for both AA6061 and Low carbon steel. Both the materials sheets were cut in 0°, 45°, and 90° rolling directions. For each set of rolling direction, 3 specimens are cut, in total 18 specimens tested. To find anisotropy constants, the specimens are cut in different rolling directions of the sheet material such as 0°, 45° and 90°, 9 specimens were tested. The tensile test specimens before and after the tension test are shown in Fig. 4.1. From the Fig.4.1, none of the samples were failed in the gripping zone and also all the specimen's failure phenomenon is similar. The test result is extracted in the form of the force-elongation data. By which stress-strain graphs are developed for extracting the mechanical properties. The full details of mechanical properties extraction have been discussed in the followed section.

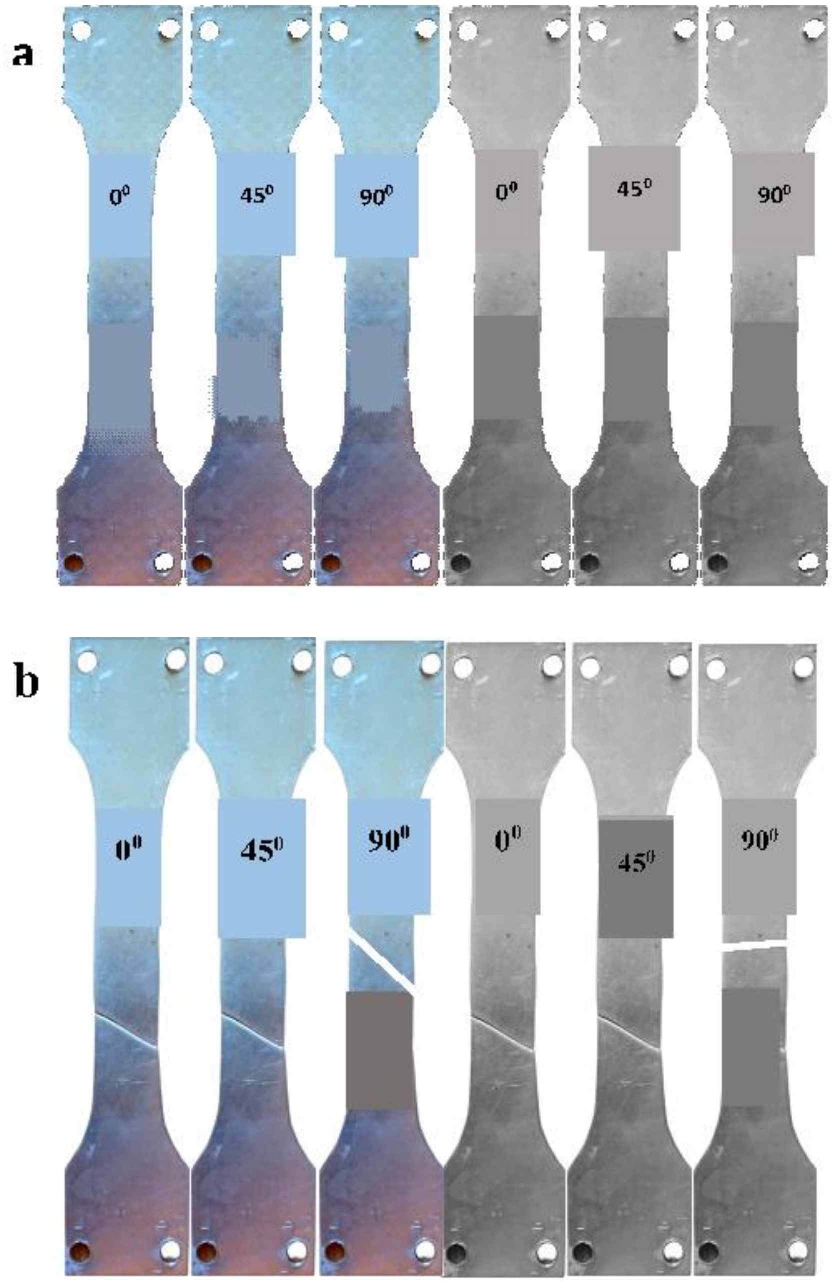

Figure 4. 1: Tensile Test specimens, a) before the test and b) after the test

4.1.2 Stress- strain

From the force and elongation data obtained from the tensile tests, engineering stress, engineering strain, true stress and true strain are calculated using equations 3.1, 3.2, 3.3, and 3.4 respectively. These evaluations are made for three rolling directions (0°, 45°, and 90°). For illustration, stress-strain plots are shown in Fig. 4.2 and 4.3 for AA 6061 alloy and low carbon steel. The extracted mechanical properties are yield strength, ultimate tensile strength (UTS) strength coefficient (K) and 'n' values. All of these results are tabulated in Table 4.2 and Table 4.3 shown below.

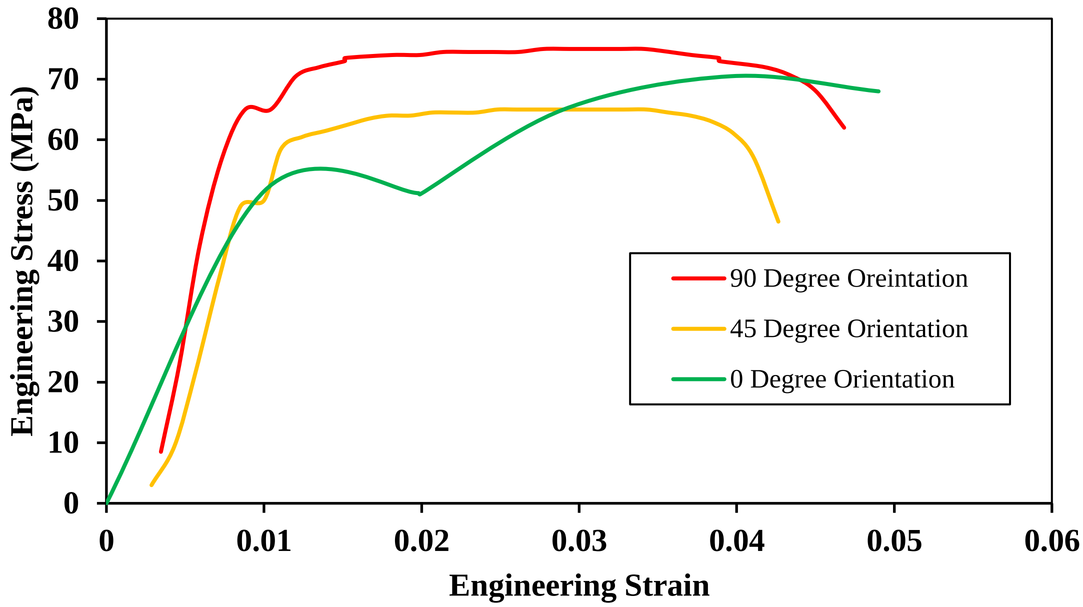

Figure 4. 2: Stress-Strain plot for AA6061 alloy

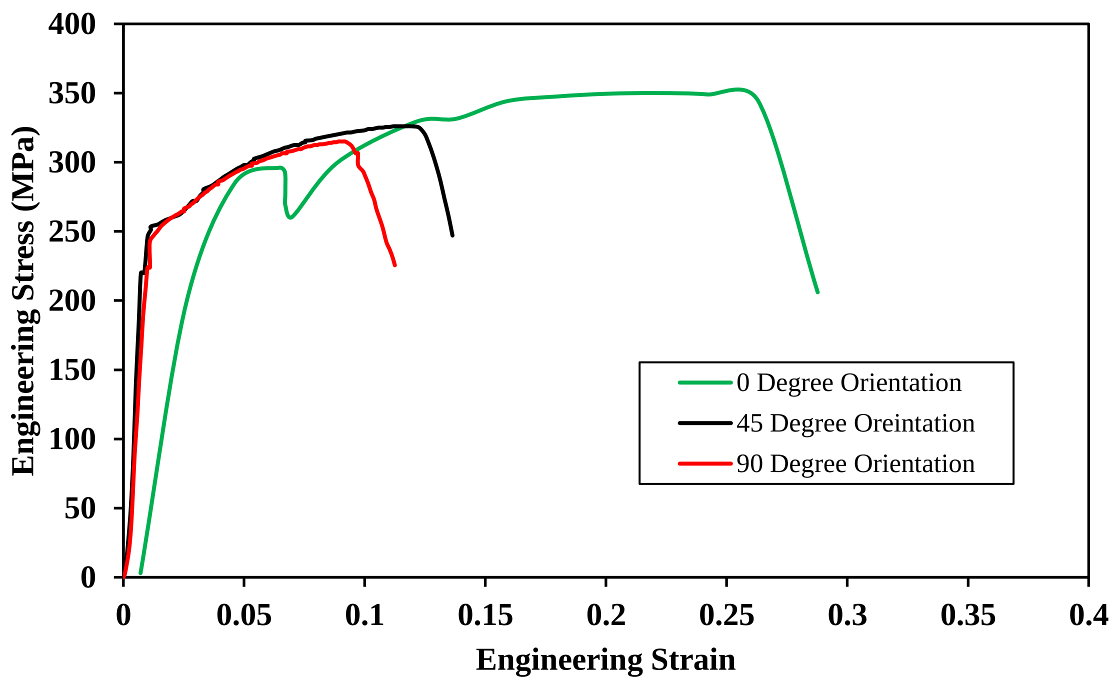

Figure 4. 3: Stress-Strain plot for Low- Carbon steel

Figure 4.2 and 4.3 show the engineering stress-strain curve of AA6061 and low carbon steel respectively. The variations in the stresses and strains are seen for the different rolling directions for AA6061 and low carbon steel. The behavior phenomenon is seen as 90^0 has better behavior and followed by 90^0 and 0^0 for AA6061 sheet and 0^0 has better behavior and followed by 90^0 and 45^0 in Low – carbon steel sheet. As it can be seen from the graphs, the stress- strain relations are not consistent with the angle to rolling directions; this is due to calibration errors and geometric accuracy of the prepared tensile specimens.

4.1.3 Plastic strain ratio

Equation 3.23 is used to calculate the plastic strain ratio (r) manually by measuring the change in axial gage length and the change in width. In this approach, prior to testing the specimen is marked along length and width direction with reference to center point shown in the Fig. 4.4 with 10mm distance; width and distance between gage marks is measured with calipers. The specimen is then pulled to a strain less than at maximum force (before onset of necking) up to 10 % elongation – and then unloaded. The final width and gage length are then measured to determine r-value.

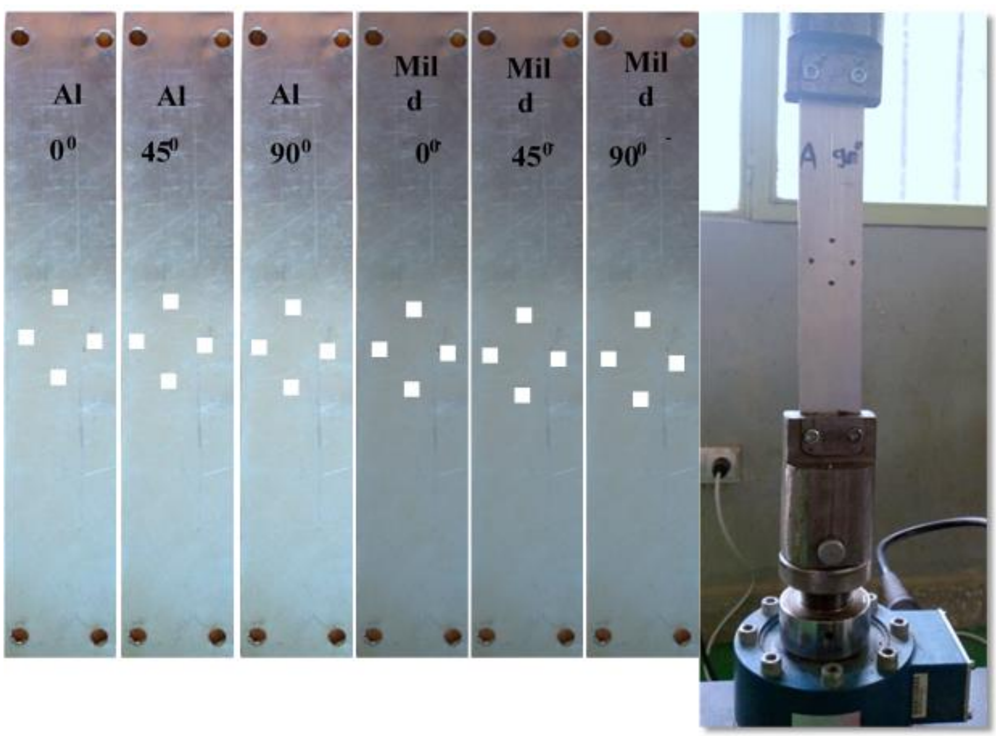

Figure 4. 4: AA6061 and low carbon steel specimens for r-value test (left), example of testing procedure – base material (Al-sheet) (right)

The entire mechanical behavior of both the sheets indicated in the Table 4.2 and 4.3. Using the r-values in the three directions (0^0, 45^0, and 90^0 to the rolling direction), two other important parameters – planar anisotropy parameter (Δr) and normal anisotropy parameter (r_m) – are calculated using equation 3.25 and 3.26 respectively. Planar anisotropy parameter (Δr) is an indicator of the ability of a material to demonstrate a non-earing behavior and it is preferred to be as small as possible. On the other hand, Normal anisotropy parameter (r_m) is an indicator of the ability of a material to be deep drawn and it is preferred to be as high as possible. Table 4.4 shows these values for AA6061 and low carbon steel sheet materials.

Table 4. 2: Mechanical properties of the AA 6061 alloy sheet metal

Orientation	Yield stress [MPa]	Ultimate tensile strength [MPa]	Material constant (K) [MPa]	Hardening exponent (n)	Lankford's coefficient r	Total Elongation (%)
A0D1	83	150	125	0.891	0.8365	
A0D2	110	164	129	0.910	0.874	
A0D3	97	169	133	0.9064	0.901	4.9888
Average	**97±0.33**	**161±0.04**	**129±0.02**	**0.9025±0.02**	**0.871±0.08**	**4.9888**
A45D1	87	157	126.545	0.1452	0.88987	2.611
A45D2	92	149	139	0.0691	0.798	2.8602
A45D3	86	161	141	0.0546	0.842	2.6514
Average	**88±0.02**	**156±0.03**	**135±0.04**	**0.0896±0.05**	**0.84±0.12**	**2.707533**
A90D1	85	162	176	0.0654	0.820	2.109
A90D2	91	158	189	0.0786	0.756	2.744
A90D3	101	153	168	0.0759	0.799	2.4676
Average	**92±0.06**	**158±0.02**	**177±0.04**	**0.073±0.02**	**0.792±0.08**	**2.4402**
Grand Average	**92±0.14**	**158±0.03**	**147±0.034**	**0.3564±0.03**		**3.3788**

Table 4. 3: Mechanical properties of the low carbon steel sheet metal

Orientation	Yield stress [MPa]	Ultimate tensile strength [MPa]	Material constant K [MPa]	Hardening exponent n	Lankford's coefficient r	Total Elongation %
S0D1	315.061	350	846.66	0.3978	1.8	17.69
S0D2	258.13	260	462.16	0.2254	1.79	15.08
S0D3	210.5	211.1	359.2	0.2043	1.74	16.78
Average	**261.2±0.5**	**273.7±0.66**	**556±1.35**	**0.276±0.095**	**1.78±0.06**	**16.51**
S45D1	266.63	326	566.456	0.1974	1.6	9.53
S45D2	279.28	312.5	588.98	0.2619	1.58	17.59
S45D3	206.7	276	504.7	0.2447	1.61	16.76
Average	**250.8±0.35**	**304.8±0.18**	**553.4±0.17**	**0.2347±0.032**	**1.6±0.05**	**14.63**
S90D1	265.859	315	547.685	0.1887	1.98	7.354
S90D2	268.1	276.5	441.465	0.1681	1.81	13.13
S90D3	244.58	271.5	493.34	0.2326	1.79	12.98
Average	**259.5±0.1**	**287.67±0.16**	**494.16±0.12**	**0.1965±0.04**	**1.86±0.1**	**11.16**
Grand Average	**267.2±0.3**	**288.73±0.33**	**534.51±0.55**	**0.2357±0.05**		**14.1**

Table 4. 4: Planar anisotropy parameter (Δr) and Normal anisotropy parameter (rm) values

Material	***Planar anisotropy parameter (Δr)***	***Normal anisotropy parameter (r_m)***
AA6061	0.01	0.836
Low carbon steel	0.22	1.71

From the results tabulated in table 4.4, it is observed that low – carbon steel sheet has high earing tendency and deep drawability than that of AA6061 sheet metal as the planar and normal anisotropy values are higher for low – carbon steel sheet.

4.2 Deep drawing experiments using Universal testing machine

Based on the formula given by Groover, (2010), the size of the circular sheet blank is selected. The diameter of the blank is 90mm. in order to understand the effect of the blank holding force on earing, conventional deep drawing experiments were conducted using universal testing machine WP310, ASTU. These experiments are conducted at testing Laboratory of ASTU. Since this machine not compatible to perform the deep drawing operations, customized deep drawing setup designed and manufactured in terms of die, blank holder, and punch. The main missing parts are height reading sensor, blank holding force reader and the connection between these two with the computer. Due to the above-mentioned main reasons, the objectives of doing conventional deep drawing experiment in this work is changed to make cup shaped products are possible. By which the experiments presented in this thesis shows that it is possible to design and manufacture deep drawing setup and produce different products by this process.

The punch diameter is chosen as 48mm and the die diameter is 51.1mm. The fillet radii of punch and die are 6 and 8mm respectively. During the experiment, different values of blank holding force are used. Hydraulic oil is used as a lubricant throughout the experiment. This friction coefficient value is taken from the previous work of (Lăzărescu & Banabic, 2017). In order to obtain blank holder force, four nuts are placed around the blank between the die and blank holder. Without blankholder force, the wrinkling in the flange region takes place freely. At first steps, free wrinkling is observed, moreover when the wave amplitudes become higher than the nut height due to increased punch depth, blank holder force is applied to the blank so that the defects reduced. Some of the deep drawn products which have defects are shown in the appendix A. WP 310 testing machine is shown in Fig 3.10. The specifications of the testing machine are given in Appendix B.

After performing many experimental trials, the AA6061 material failed to produce good products. The output of the AA6061 is full of defects like wrinkling, tearing, crack, shearing and so on. Following the same procedure, the low carbon steel gave wrinkling free cup. With all missing parts, through many trials experiment, one thing can surely be concluded which is when the blank holding force increases wrinkling is eliminated and other defects appear like tearing, and when the BHF decrease from the optimum value, wrinkling defect is observed. The deep drawn parts with different blank holder force values are illustrated in Fig. 4.5.

Figure 4. 5: Deep drawn cups with different blank holding force; fig. a & d shows deep drawn cup for AA6061 and fig. c & b shows deep drawn cup for Low-carbon steel sheet

Based on the difficulties of deep drawing process, simulation is performed with the same conditions by using the obtained mechanical properties.

4.3 Simulation of deep drawing process

The FE simulations of deep drawing were conducted using BHFs of 1kN and 50kN, respectively for both AA6061 and low carbon steel. It was observed that wrinkling occurred when the BHF was not enough to prevent the buckling of the blank sheet, and tearing appeared due to the insufficient material flow when the BHF is excessive. Next, the predictions of earing in deep drawing using various uniform BHFs of 1kN, 5kN, 10kN, 15kN, 20kN, 25kN, 30kN, 35kN, 40kN, 45kN and 50kN are carried out, after the simulations, for the low carbon steel, it is observed that wrinkling occurred when the blank holder forces bellow 20kN and as the BHF goes above 20kN, it generates challenges for the blank material to flow into the die, the earing profile graphs for 15kN, 20kN and 25kN are shown in Fig. 4.6. And for the AA6061, it is observed that wrinkling occurred at BHFs are bellow 9kN and as the BHF goes above 9kN, it produces challenges for the blank material to flow into the die, the earing profile graphs for 6kN, 9kN and 14kN are shown in Fig. 4.7. The present FEA showed that the height of the deep-drawn cup monotonically increases from 15kN to 25kN for low carbon steel and 6kN to 14kN for the AA6061 alloy material. The results revealed that the height of earing, the peaks of the waves shown in Fig. 4.7 and 4.5, increased when the BHF increased. A significant increase of earing height was observed at high BHF.

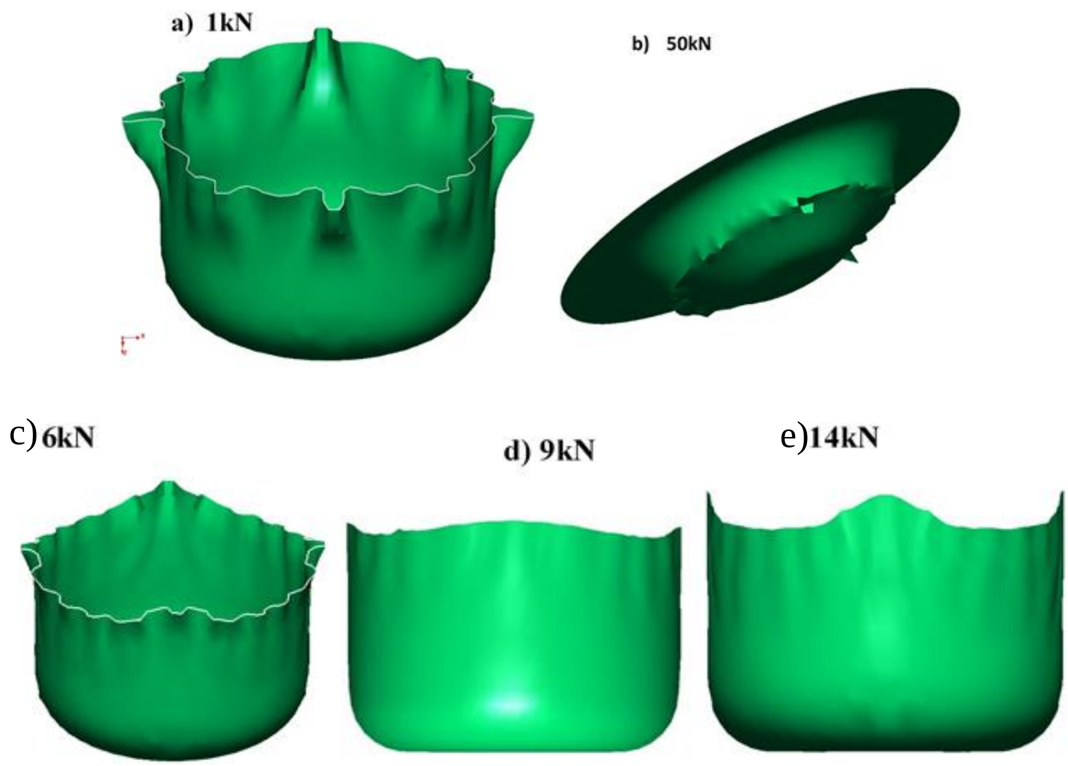

Figure 4. 6: FE simulation of the deep-drawn cup of AA6061 using uniform BHFs of (a) 1kN, (b) 50kN, (c) 6 kN, (d) 9kN, and (e) 14kN

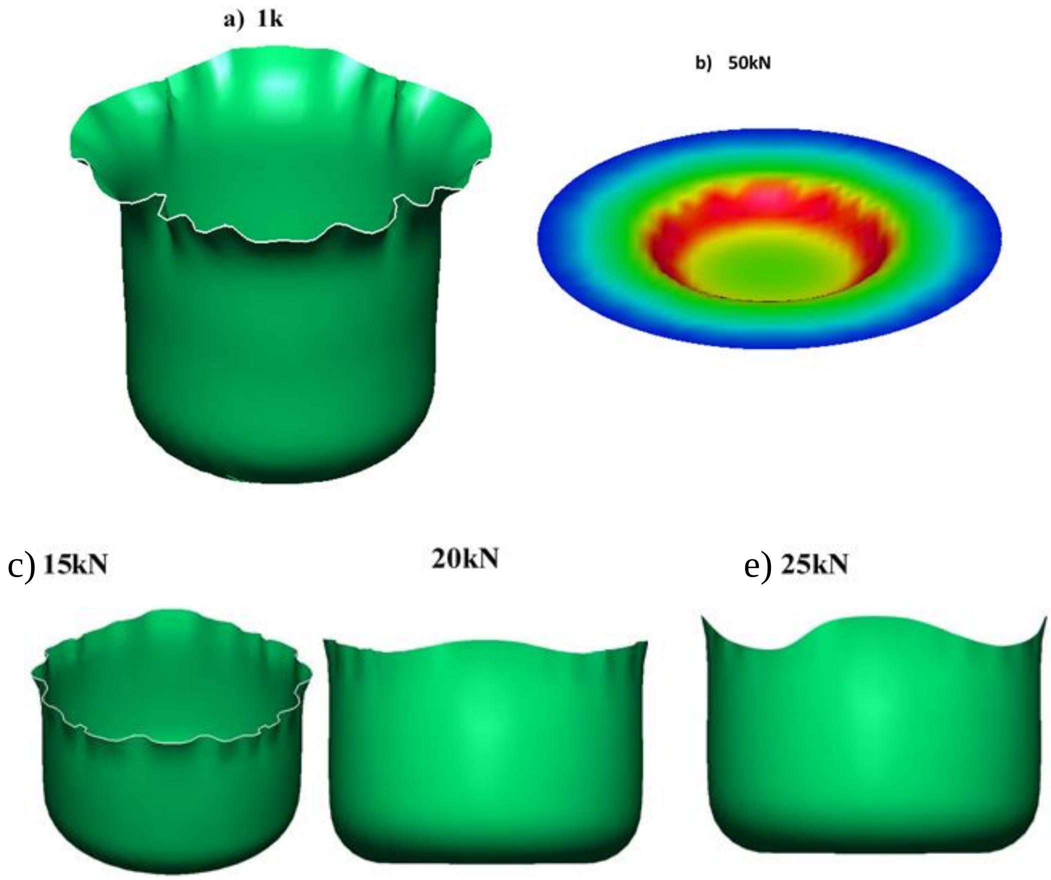

Figure 4. 7: FE simulation of the deep-drawn cup of low carbon steel using uniform BHFs of (a) 1kN, (b) 50kN, (c) 15 kN, (d) 20kN, and (e) 25kN

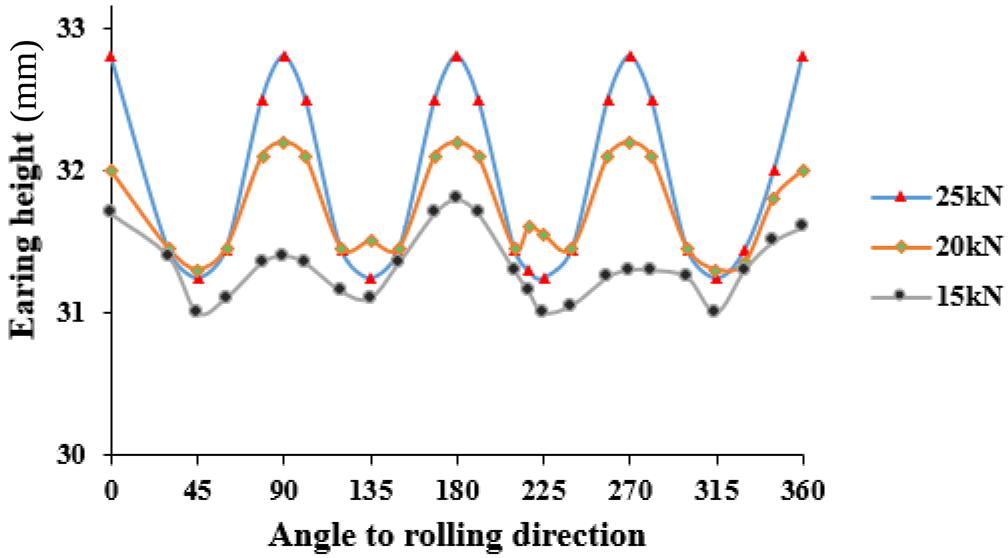

Figure 4. 8: Earing height profiles of low carbon steel using the present finite element analysis (FEA) with uniform BHFs of 15kN, 20kN, and 25kN

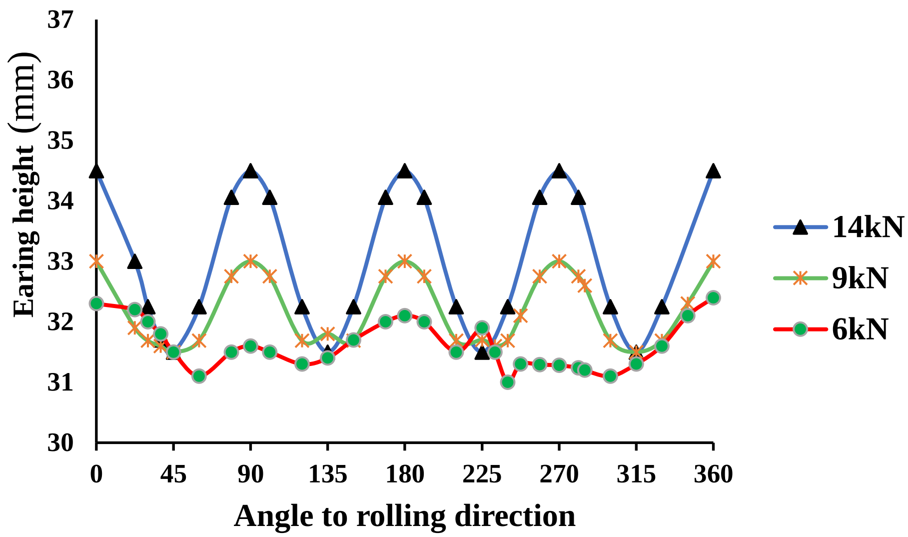

Figure 4. 9: Results of the earing height profiles of AA6061 using the present finite element analysis (FEA) with uniform BHFs of 6kN, 9kN, and 14kN

The number of the blank holding force required are selected to be three BHFs for both materials. However, many more analysis were conducted by varying the blank holding forces which reduces wrinkling first and then earing phenomenon then tearing. The blank holding forces varied are as shown it the Table 4.5 below.

Table 4. 5: Blank holding forces used in this work

	AA6061 alloy			Low carbon steel		
Blank holding force (kN)	6	9	14	15	20	25
	1, 5, 10, 15, …., 50			1, 5, 10, 15, ……., 50		

The range 1 – 50kN is inspected thoroughly for both materials and wrinkling is observed at blank holder force lower than 9kN for AA6061 alloy and 20kN for low carbon steel and failures are occurred above BHF of 9kN for AA6061 alloy and 20kN for low carbon steel due to tearing, cracking and others. The effect of wrinkling (due to insufficient blank holding) on the final shape can be visualized in Fig.4.5(a) and 4.7(a), and also at the appendix A.

Figure 4.5 and 4.7 depicts the resulting blank shapes of five separate analysis for each material with 1, 6, 9, 14, and 50kN for AA6061 alloy and 1, 15, 20, 25, and 50kN for low carbon steel. All other process and simulation parameters with their material properties are kept constant.

For AA6061 alloy, in the 9kN case, almost no wrinkling is observable, whereas the 1 and 6kN wrinkles. In this figure, the wrinkling waves of the low force case are visually observable without argument. And the same phenomenon has happened for low carbon steel; in the 20kN case, no wrinkling is observed and wrinkling is observed for BHFS of 1 and 15kN.

4.3.1 Discussion of the simulation results

First, the FE simulations of deep drawing were conducted using BHFs of 1kN and 50kN, respectively. It was observed that wrinkling occurred when the BHF was not enough to prevent the buckling of the blank sheet, and tearing appeared due to the insufficient material flow when the BHF was excessive (Han et al., 2013). Next, the determination of earing in deep drawing using various uniform BHFs of 6kN, 9kN, and 14kN for AA6061 alloy and 15kN, 20kN and 25kN for Low - Carbon steel sheets were carried out, as shown in Figure 4.9 and fig 4.8 respectively. The present FEA showed that the height of the deep-drawn cup monotonically decreases from 0° to 45° to the RD and monotonically increases from 45° to 90° to the RD. This is due to the contribution of the yield stress directionality(Yoon et al., 2011). As the planar anisotropy was positive (for AA6061, Δr = 0.01 and for Low - Carbon steel, Δr = 0.22), the formation of earing was observed at 0° and 90° to the RD, which well correlated with the theoretical analysis (Hu, 2001). It can be seen that four main ears formed at 0°, 90°, 180°, and 270° in the cup deep drawing process. This is partially attributed to the slower flow of sheet metal into the die cavity in these regions than in the other ones. The results show that the uniform BHFs of 9kN and 14kN for AA6061 alloy, and 20kN and 25kN for Low - Carbon steel exhibited bigger ears at 0° and continues to show with 90^0 gaps. Meanwhile, the uniform BHF of 6kN for AA6061 and 15kN for Low - Carbon steel exhibited very small earing profile at 0°, 90°, 180°, and 270°. The results revealed that the height of earing, the peaks of the waves shown in Fig 4.9 and 4.8, increased when the BHF increased. A significant increase of earing height was observed at 0°, 90°, 180°, and 270°. with the larger BHF. By using equation (3.27), the % ear height variation, can then be determined. This result illustrates that the ΔH also increased with the increase in BHF.

4.3.2 Discussion of the experimental results

After assembling the manufactured circular deep drawing setups on the available UTM machine at ASTU lab, experimentation of many circular blank deep drawn product is conducted. To increase or decrease the blank holding force, bolt and nut mechanism is used. As the nut is tightened to the bolt then the tearing phenomenon is increased. This was due to the increament to blank holding force; and as the nut is loosen to the bolt then the wrinkling phenomenon is increased. This was due to the decrement to the blank holding force. After conducting repetitive tightening and loosening work on the bolt nut mechanism, wrinkling and tearing free deep drawn cup is produced. Therefore, the best result found through the repetitive circular deep drawing experimental work is a cup with maximum height of 36.3mm and minimum height of 35.9mm for low- carbon steel sheet; and maximum height of 34.2mm and minimum height of 33.9mm. This result also showed the deep drawability and earing tendency of the low – carbon steel sheet is higher than that of AA6061 sheet.

4.3.3 Cup height and %earing height

The cup heights were measured at different points with respect to width as shown in the Fig. 3.9. Height versus width data's are found at appendix C. Variation of cup height is better observed in terms % ear height where % ear height is calculated using equation. (3.15). The percentage of earing with respect to the selected blank holding force are shown in the Table 4.6.

Table 4. 6: Variation of Earing of AA6061 and low carbon steel cups with varying blank-holding force (other parameters kept constant)

Material	Blank holding force (kN)	Earing %
AA6061 alloy	6	2.52
	9	2.88
	14	4.96
Low carbon steel	15	4.52
	20	6.45
	25	9.52

For the AA6061 alloy, among all the three blank holding forces, the smallest cup height is found under blank holder force of 6kN. Although, BHF of 6kN show good result of earing, it also shows high or observable amount of wrinkling. When the BHF is 14kN, the earing is increased by 2.44%. but when the BHF is 9kN, optimized earing is observed and wrinkling is reduced. For the low carbon steel, BHF of 15kN shows 4.52% earing which is the smallest among others and also shows high wrinkling defect. BHF of 25kN shows 9.52% earing which is the highest among others and; BHF of 20kN provide with intermediate value of earing and reduced wrinkling.

From the table 4.6, the low carbon steel shows high amount of earing when it is compared with the AA6061 alloy. This is due to the plastic anisotropic properties of the low carbon steel as shown in the Table 4.4. It was, thus, observed that blank holder force significantly affects the cup height and quality of the deep drawn cup of both AA6061 and low carbon steel. This result illustrates that the earing height also increased with the increase in BHF.

Chapter Five

5. Conclusion and Recommendation

In the present study, investigating the effect of blank holding force (BHF) on earing defect by using finite element analysis and experimentation was proposed in the circular deep drawing process of AA6061 and low carbon steel sheets. The following conclusions of this study can be summarized as follows:

i. Circular blank with diameter of 90mm was designed.
ii. Tensile testing is conducted to determine the mechanical properties of the materials.
iii. Numerical simulation of deep drawing process is done with blank holder force of 1- 50kN using Pamstamp 2G software.
iv. Drawing setups are designed and manufactured.
v. Deep drawing experiment is conducted with varying blank holder force.
vi. The present study revealed that the blank holding force of 9 and 20kN for AA6061 and Low- carbon steel sheets respectively have showed a noticeable earing height reduction by 2.08% and 3.07%. the simulated result also showed when the blank holder force is below 9 and 20kN, the wrinkling is increased and when it is above 9 and 20kN, tearing phenomenon is increased for both AA6061 and Low- carbon steel sheet respectively.
vii. The experimental result showed higher tendency of earing for Low-carbon steel than AA6061 as the planar anisotropy (AA6061, $\Delta r = 0.11$ and $\Delta r = 0.22$) and the deep drawability of Low-carbon steel is greater than AA6061 as it is given by the normal anisotropy (AA6061, $r_m = 0.836$ and Low-carbon steel, $r_m = 0.836$).

Earing is the result of the effects of different deep drawing process parameters. Hence, it is recommended that studying the effect of multi variables with respect to earing defect is recommended for future work.

Reference

Ghosh A. and Mallik A. K.,(2011). “Manufacturing Science”, 2nd Edition, Affiliated East West Press, p. 562, ISBN: 812034426X. 9788120344266

R. Patel, H. Dave, and H. Raval, “Study of earing defect during deep drawing process with finite element simulation,”(2015). Key Eng. Mater., vol. 639, no. 3, p. pp 91-98, doi: 10.4028/www.scientific.net/KEM.639.91.

P. Das, S. K. Panda, and D. K. Pratihar,(2013). “Modification of Initial Blank Shape to Minimize Earing in Deep Drawing Process,” Int. J. Adv. Mater. Manuf. Charact., vol. 3, no. 1, pp. 99–104, doi: 10.11127/ijammc.2013.02.018.

P. S. Nagda, P. S. Bhatt, and M. K. Shah, (2017).“Finite Element Simulation of Deep Drawing Process to Minimize Earing,” World Acad. Sci. Eng. Technol. Int. J. Mech. Mechatronics Eng., vol. 11, no. 2, pp. 413–416.

O. O. Oluwole1*, C. O. Anyaeche2, and O. V. Faola3,(2010) “Effect of Draw Ratio and Sheet Thickness on Earing and Drawability of Al 1200 Cups,” Miner. Mater. Charact. Eng., vol. 9, no. 5, pp. 461–470.

Han, Jing, Koetsu Yamazaki, Shinya Makino, and Taketo Shirasawa.(2013). "Optimization of deep drawing process for circular cup forming." In 10th World Congress on Structural and Multidisciplinary Optimization May, vol. 19, p. 24.

J. Srirat, S. Kitayama, and K. Yamazaki,(2012). “Optimization of initial blank shape with a variable blank holder force in deep-drawing via sequential approximate optimization,” J. Adv. Mech. Des. Syst. Manuf., vol. 6, no. 7, pp. 1093–1106, doi: 10.1299/jamdsm.6.1093.

K. M. Younis and A. Sh.Jaber,(2018) “Experimental and Numerical Study of the Earing Defect During Square Deep Drawing Process,” Eng. Technol. J., vol. 36, no. 12, doi: 10.30684/etj.36.12a.8.

D. K. Muhsin Younis * and A. Shbeeb Jaber,(2011). “Experimental and theoretical study of interaction,” Eng. Tech. J., vol. 29, no. 12, pp. 1143–1152.

Dixit, R. K. S. P. M. (2009). Finite element simulation of earing defect in deep drawing. Int J Adv Manuf Technol, 45(27, Feb), 219–233. https://doi.org/10.1007/s00170-009-1963-5

Reddy, P. V., Ramulu, P. J., Madhuri, G. S., Govardhan, D., & Prasad, P. V. S. R. (2016). Design and Analysis of Deep Drawing Process on angular Deep Drawing Dies for Different Anisotropic Materials. IOP Conference Series: Materials Science and Engineering, 149(1). https://doi.org/10.1088/1757-899X/149/1/012142

Gharib, H., Wifi, A. S., Younan, M., & Nassef, A. (2006). Optimization of the blank holder force in cup drawing. Journal of Achievements in Materials and Manufacturing Engineering, 18(1–2), 291–294.

Devendar, G., & Reddy, A. C. (2016). Deep Drawing Process Parameters: A Review. International Journal of Scientific & Engineering Research, 7(6 June). https://doi.org/10.14741/ijcet/22774106/6.4.2016.20

JOSHI, 1A. R., KOTHARI, 2K. D., & Dr. JHALA, 3R. L. (2013). Effects Of Different Parameters On Deep Drawing Process: Review. International Journal of Engineering, Research and Technology (IJERT), 2(3, March).

Groover, M. P. (2010). Fundamentals of Modern Manufacturing (4th ed.). JOHN WILEY & SONS, INC. https://doi.org/10: 987654321

Ohwue, T., & Kobayashi, Y. (2014). Analysis of earring in circular-shell deep-drawing of bcc and hcp sheet metals. Procedia Engineering, 81(October), 887–892. https://doi.org/10.1016/j.proeng.2014.10.093

Desai, S. G., Pardeshi, R. H., & Date, P. P. (2005). Study of various initial blank shapes to minimize the earing in the different shaped formed parts using finite element analysis. AIP Conference Proceedings, 778 A(2005), 855–860. https://doi.org/10.1063/1.2011329

Athale, M., Gupta, A. K., Singh, S. K., & Vaidyanathan, A. (2017). Analytical and finite element simulation studies on earing profile of Ti-6Al-4V deep drawn cups at elevated temperatures. International Journal of Material Forming, 11(24, May), 479–490. https://doi.org/10.1007/s12289-017-1358-3

Yoon, J. W., Dick, R. E., & Barlat, F. (2011). A new analytical theory for earing generated from anisotropic plasticity. International Journal of Plasticity, 27(8), 1165–1184. https://doi.org/10.1016/j.ijplas.2011.01.002

Trzepieciński, T., & Gelgele, H. L. (2010). Investigation of anisotropy problems in sheet metal forming using finite element method. International Journal of Material Forming, 4(25, Aug), 357–369. https://doi.org/10.1007/s12289-010-0994-7

Wang, H., Men, M., Yan, Y., Wan, M., & Li, Q. (2019). Prediction of Eight Earings in Deep Drawing of 5754O Aluminum Alloy Sheet. Chinese Journal of Mechanical Engineering (English Edition), 32(1). https://doi.org/10.1186/s10033-019-0390-2

Gürün, H., & Karaaɫaç, I. (2015). The experimental investigation of effects of multiple parameters on the formability of the DC01 sheet metal. Strojniski Vestnik/Journal of Mechanical Engineering, 61(11), 651–662. https://doi.org/10.5545/sv-jme.2015.2562

Adams, W. S., Savran, D., Maran, S. P., & Kinney, A. L. (2018). Deep drawing mechanism, parameters, defects and recent results: state of the art. IOP Conference Series: Materials Science and Engineering, 146(1). https://doi.org/10.1088/1757-899X/463/1/011002

Patel, R., Dave, H., & Raval, H. (2015). Study of earing defect during deep drawing process with finite element simulation. Key Engineering Materials, 639(3), pp 91-98. https://doi.org/10.4028/www.scientific.net/KEM.639.91

Lăzărescu, L., & Banabic, D. (2017). Evaluation of deep drawing force under different friction conditions. MATEC Web of Conferences, 137, 0–7. https://doi.org/10.1051/matecconf/201713705003

Khairnar, Y. S., Deshmukh, D., Dhembre, K., Sawant, G., & Bhosale, A. (2018). Review on Optimization of process parameter in square shaped components in deep drawing process . Journal of Mechanical and Civil Engineering (IOSR-JMCE), 30–34.

Hutchinson, B. (2015). Critical assessment 16: Anisotropy in metals. Materials Science and Technology (United Kingdom), 31(12), 1393–1401. doi.org/10.1179/1743284715Y.0000000118

Engler, O., Aegerter, J., & Calmer, D. (2020). Control of texture and earing in aluminium alloy AA 8011A-H14 closure stock. Materials Science and Engineering A, 775(October 2019), 138965. https://doi.org/10.1016/j.msea.2020.138965

Ahmetoglu, M. A., Altan, T., & Kinzel, G. L. (1992). Improvement of part quality in stamping by controlling blank-holder force and pressure. Journal of Materials Processing Tech., 33(1–2), 195–214. https://doi.org/10.1016/0924-0136(92)90319-N

D.Younis, D. A. (2010). The effect of drawing ratio in deep drawing process on thickness distribution along the cup. AL-Rafdain Engineering Journal (AREJ), 18(4), 81–86. https://doi.org/10.33899/rengj.2010.31547

Lange, Kurt.(1985). "Handbook of metal forming." McGraw-Hill Book Company, 1985, pp,1216,1985, doi: 10.1007/BF02834383

Hoffman, H., ed. (1998). Metal Forming Handbook. Springer Science & Business Media, 1998, doi: 10: 1007/978-3-642-58857-0, ISBN: 978-3-642-58857-0.

Fallahiarezoodar, T. Mao, and T. Altan,(2014). “Using limiting draw ratio to evaluate material drawability, Part I Concepts and testing parameters,” Stamp. J., no. June, pp.12.13.

S. GambH, “Hydraulic Universal Material Tester, 50 kN.” WP 310. 2014, [Online]. Available: http://www.selkagambh.com.

D. P. R. Palaparti, B. K. Choudhary, E. I. Samuel, V. S. Srinivasan, and M. D. Mathew,(2012) “Influence of strain rate and temperature on tensile stress – strain and work hardening behaviour of 9Cr – 1Mo ferritic steel,” Mater. Sci. Eng. A, vol. 538, pp.110.117.

Kaftanoğlu, B.,(1973) "Determination of Coefficient of Friction under Conditions of Deep Drawing and Stretch Forming", Presented at the First World Conference on Industrial Tribology, Dec. 11-18, 1972, New Delhi, India. Also, Wear, 25 (1973), 177-188.

Yalçın, S. (2010). Analysis and modeling of plastic wrinkling in deep drawing (Master's thesis, Middle East Technical University).

Ohwue, T., & Kobayashi, Y. (2014). Analysis of earring in circular-shell deep-drawing of bcc and hcp sheet metals. Procedia Engineering, 81(October), 887–892. https://doi.org/10.1016/j.proeng.2014.10.093

Singh, A., Basak, S., Lin, L. P., Roy, G. G., Jha, M. N., Mascarenhas, M., & Panda, S. K. (2018). Prediction of earing defect and deep drawing behavior of commercially pure titanium sheets using CPB06 anisotropy yield theory. Journal of Manufacturing Processes, 33(September), 256–267. https://doi.org/10.1016/j.jmapro.2018.05.003

Demirci, H.I.; Esner, C.; Yasar,(2008). M. Effect of the blank holder force on drawing of aluminum alloy square cup: Theoretical and experimental investigation. J. Mater. Process. Technol., 206, 152–160, doi:10.1016/j.jmatprotec.2007.12.010.

Hu, P.; Liu, Y.; Wang, J.(2001). Numerical study of the flange earring of deep-drawing sheets with stronger anisotropy. Int. J. Mech. Sci. 43, 279–296, doi:10.1016/s0020-7403(99)00119-8

APPENDICES

Appendix A

A. Deep drawing experimental results

Figure A. 1: deep drawn cup products with different blank holding force

Appendix B

Hydraulic Universal Material Tester, 50kN

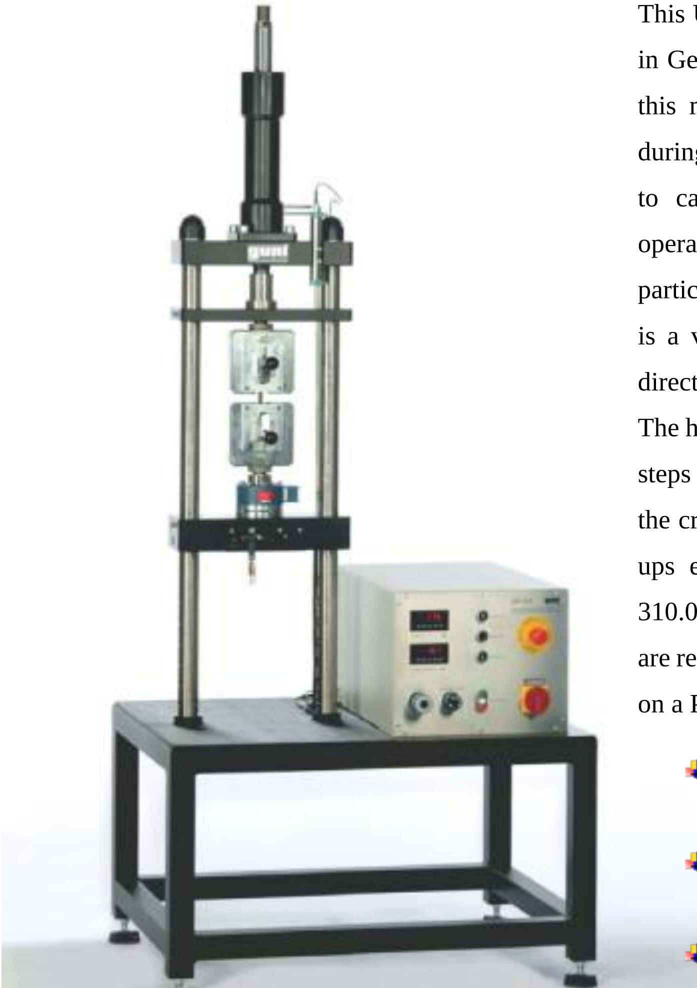

Figure 1: WP 310 UTM

This UTM is manufactured by gunt humburg company in German. Due to the clear, straightforward layout of this materials tester, tests can be observed in detail during all phases. The capacity of the tester is sufficient to carry out tests of an industrial nature. Simple operation and robust construction make the tester particularly suitable for student experiments. The tester is a vertical, hydraulically operated pillar tester with direct generation of both tensile and compressive forces. The height of the lower crossmember can be adjusted in steps for coarse adjustment. Cylindrical receptacles on the crossmembers make the different experimental set-ups easy to change, e.g. wedge grips (accessory P 310.05, as shown in pic. left). Force and displacement are recorded by sensors, displayed and can be processed on a PC.

- Hydraulically operated pillar tester with direct generation of force
- Both tensile and compressive forces can be generated
- Test force in both directions 50kN
- Digital force and displacement display
- UNT software for data acquisition

Technical Data

Working area, WxH: 300x925mm

Hydraulic test force generation

- test force: 0...50kN

- max. system pressure: 175bar

- max. piston stroke: 150mm

Dimension and weight: Weight: approx. 380kg

LxWxH:1.050x800x2.300mm

Gear pump

- max. flow rate: 1cm³/rotation

- power consumption: 0,55kW

Measuring ranges

- force: 0...50kN

- displacement: 0...150mm

LED displays- measurement repetition rate: 2,5s-1

- 6 digits

Appendix C

Low-carbon steel material

Table C. 1:Cup height Vs angle to rolling direction at 25kN

Cup height	Angle to rolling direction
34.5	0
33	22.5
32.25	30
31.701	37.5
31.5	45
32.25	60
34.0607	78.75
34.5	90
34.0607	101.25
32.25	120
31.5	135
32.25	150
34.0607	168.75
34.5	180
34.0607	191.25
32.25	210
31.5	225
32.25	240
34.0607	258.75
34.5	270
34.0607	281.25
32.25	300
31.5	315
32.25	330
34.5	360

Table C. 2: Cup height Vs angle to rolling direction at 15kN

Cup height	Angle to rolling direction
32.3	0
32.2	22.5
32	30
31.8	37.5
32.5	45
31.1	60
31.5	78.75
31.6	90
31.5	101.25
31.3	120
31.4	135
31.7	150
32	168.75
32.1	180
32	191.25
31.5	210
31.9	225
31.5	232.5
31	240
31.3	247.5
31.29	258.75
31.28	270
31.24	281.25
31.2	285
31.1	300
31.3	315
31.6	330
32.1	345
32.4	360

Table C. 3: Cup height Vs angle to rolling direction at 20kN

Cup height	Angle to rolling direction
32.3	0
32.2	22.5
32	30
31.8	37.5
32.5	45
31.1	60
31.5	78.75
31.6	90
31.5	101.25
31.3	120
32.4	135
31.7	150
32	168.75
32.1	180
32	191.25
31.5	210
31.9	225
31.5	232.5
31	240
31.3	247.5
31.29	258.75
31.28	270
31.24	281.25
31.2	285
31.1	300
31.5	315
31.6875	330
32.3	345
33	360

AA6061 material

Table C. 4: Cup height Vs angle to rolling direction at 14kN

Cup height	Angle to rolling direction
32.8	0
31.45	30
31.25	45
31.45	60
32.5	78.75
32.8	90
32.5	101.25
31.45	120
31.25	135
31.45	150
32.5	168.75
32.8	180
32.5	191.25
31.45	210
31.3	217.5
31.25	225
31.45	240
32.5	258.75
32.8	270
32.5	281.25
31.45	300
31.25	315
31.45	330
32	345
32.8	360

Table C. 5: Cup height Vs angle to rolling direction at 9kN

Cup height	Angle to rolling direction
32	0
31.45	30
31.3	45
31.45	60
32.1	78.75
32.2	90
32.1	101.25
31.45	120
31.5	135
31.45	150
32.1	168.75
32.2	180
32.1	191.25
31.45	210
31.6	217.5
31.55	225
31.45	240
32.1	258.75
32.2	270
32.1	281.25
31.45	300
31.3	315
31.35	330
31.8	345
32	360

Table C. 6: Cup height Vs angle to rolling direction at 6kN

Cup height	Angle to rolling direction
32.4	0
32.1	30
31.7	45
31.8	60
32.05	78.75
32.1	90
32.05	101.25
31.85	120
31.8	135
32.05	150
32.4	168.75
32.5	180
32.4	191.25
32	210
31.85	217.5
31.7	225
31.75	240
31.95	258.75
32	270
32	281.25
31.95	300
31.7	315
32	330
32.2	345
32.3	360

Appendix D

Figure D. 1: images of single tool cutter used during machining operation